COMPUTED AND EXPERIMENTAL HUGONIOTS FOR UNREACTED POROUS HIGH EXPLOSIVES

John O. Erkman, et al

Naval Ordnance Laboratory
White Oak, Maryland

31 December 1974

NOLTR 74-213

NOL TECHNICAL REPORT

COMPUTED AND EXPERIMENTAL HUGONOITS FOR UNREACTED POROUS HIGH EXPLOSIVES

BY
John O. Erkman
David J. Edwards

31 December 1974

NAVAL ORDNANCE LABORATORY
WHITE OAK, SILVER SPRING, MD. 20910

- Approved for public release; distribution unlimited

NAVAL ORDNANCE LABORATORY
WHITE OAK, SILVER SPRING, MARYLAND 20910

UNCLASSIFIED

SECURITY CLASSIFICATION OF THIS PAGE *(When Data Entered)*

REPORT DOCUMENTATION PAGE		READ INSTRUCTIONS BEFORE COMPLETING FORM
1. REPORT NUMBER NOLTR 74-213	2. GOVT ACCESSION NO.	3. RECIPIENT'S CATALOG NUMBER
4. TITLE *(and Subtitle)* Computed and Experimental Hugoniots for Unreacted Porous High Explosives		5. TYPE OF REPORT & PERIOD COVERED Final 6. PERFORMING ORG. REPORT NUMBER
7. AUTHOR(s) JOHN O. ERKMAN DAVID J. EDWARDS		8. CONTRACT OR GRANT NUMBER(s)
9. PERFORMING ORGANIZATION NAME AND ADDRESS Naval Surface Weapons Center White Oak, Silver Spring, MD 20910		10. PROGRAM ELEMENT, PROJECT, TASK AREA & WORK UNIT NUMBERS 61152N, ZR00001, ZR0130901, MAT03L00015923
11. CONTROLLING OFFICE NAME AND ADDRESS		12. REPORT DATE 31 December 1974 13. NUMBER OF PAGES 79
14. MONITORING AGENCY NAME & ADDRESS*(if different from Controlling Office)*		15. SECURITY CLASS. *(of this report)* UNCLASSIFIED 15a. DECLASSIFICATION/DOWNGRADING SCHEDULE

16. DISTRIBUTION STATEMENT *(of this Report)*

Approved for public release; distribution unlimited

17. DISTRIBUTION STATEMENT *(of the abstract entered in Block 20, if different from Report)*

18. SUPPLEMENTARY NOTES

19. KEY WORDS *(Continue on reverse side if necessary and identify by block number)*

Explosive	Ammonium Nitrate	Particle Velocity	Melting
TNT	Porosity	Computer Code	
NB-40	Hugoniot	Magnetic Gage	
RDV	Initiation	Detonation	
Tetryl	Equation-of-State	Phase Change	

20. ABSTRACT *(Continue on reverse side if necessary and identify by block number)*

A theory of the response of porous, non-reactive materials to shock has been applied to a potentially reactive material, porous TNT. The computed Hugoniots which are based on this theory were generated and confirmed by obtaining an experimental Hugoniot for TNT at a density of 0.98 g/cc. The calculated and experimental Hugoniots agree to within 2 kbar over the range 0.35 to 1.72 mm/μsec and 3.6 to 55 kbar in the particle velocity and pressure,

DD FORM 1 JAN 73 1473 EDITION OF 1 NOV 65 IS OBSOLETE
S/N 0102-014-6601

UNCLASSIFIED

SECURITY CLASSIFICATION OF THIS PAGE *(When Data Entered)*

20. Abstract

respectively. Other experimental data on TNT have been compared with our results. Computed Hugoniots are compared with both experimental and computed results found in the Russian literature for several explosives. Comparisons for six different explosives justify use of Herrmann's code (or an equivalent method) to compute Hugoniots of porous high explosives.

NOLTR 74-213

COMPUTED AND EXPERIMENTAL HUGONIOTS FOR UNREACTED POROUS HIGH EXPLOSIVES

The work described in this report was carried out under Task MAT-03L-000/R011-01-01, IR 159, Transition from Deflagration to Detonation of NAVSURWPNCEN Independent Research Program. Both computed and experimentally measured dynamic compression curves (Hugoniot curves) for unreacted TNT are presented. Also, our computations for several other porous, unreacted explosives are compared with experimental data from the Russian literature. The work shows that Hugoniots can be computed for unreacted, porous explosives. This result is important because it simplifies the determination of the sensitivity of porous, granular explosives to shock stimuli.

Julius W. Enig

JULIUS W. ENIG
By direction

TABLE OF CONTENTS

LIST OF TABLES

TABLE OF CONTENTS (Cont.)

LIST OF TABLES (Cont.)

LIST OF FIGURES

TABLE OF CONTENTS (Cont.)

LIST OF FIGURES (Cont.)

INTRODUCTION

A knowledge of the Hugoniot of unreacted explosives is required to interpret transitional phenomena in explosives and to determine the shock sensitivity of explosives[1]. For example, the Naval Surface Weapons Center Large Scale Gap Test (LSGT)[2,3] is used to determine the relative shock sensitivity of explosives. The LSGT is calibrated to give the pressure in the gap material as a function of gap length. But after a determination of the critical gap pressure for initiating detonation, the question still remains: What is the critical pressure transmitted to the test explosive? This question cannot be answered without a knowledge of the Hugoniot of the unreacted explosive.

The usual method employed to obtain the Hugoniot of a material is to perform a series of experiments which measure two of the following variables: shock velocity, particle velocity, pressure, and volume. There are two drawbacks to this approach for porous (granular) explosives. (1) Because porous explosives react very readily, it is difficult to measure any of the above variables for the unreacted state. (2) Because a new Hugoniot is needed for every density, this approach rapidly becomes expensive. However, computational methods have been developed which yield the Hugoniot of inert, porous materials when the Hugoniot of the non-porous material is known. If these computational methods can be applied to porous explosives, much work and expense can be saved.

In this study, the authors have applied these computational methods to porous TNT for a range of densities from 1.60 to 0.98 g/cc. This method was confirmed by experimentally obtaining the Hugoniot for unreacted TNT at a density of 0.98 g/cc over the range of particle velocities of 0.350 - 1.720 mm/μsec and of pressures of 3.6 - 55.0 kbar. The electromagnetic velocity (EMV) gage[4] was used in conjunction with the known Hugoniot data of the attenuator material (PMMA) to obtain the Hugoniot data for unreacted TNT at 0.98 g/cc. The EMV gage follows particle velocity as a function of time. The gage was mounted at the inert/TNT interface and responded to the particle velocity at the interface. In the pressure range (3.6 - 55.0 kbar) covered in this work, some finite induction period is required before reaction occurs in the TNT. The EMV gage leads were covered by a thin layer of mica to insulate them from any reaction products.

COMPUTATIONAL MODELS

A computational model which reproduces the response of porous materials to shock has been used by several researchers[5,6,7]. It has been usefully applied to a wide variety of materials -- metals, graphite, plastics, boron nitride and others -- all of which are non-reactive. Successful application of this model to potentially reactive materials such as porous explosives has the advantage of expediting the studies of these materials by saving much experimental effort. The model requires a knowledge of the equation of state of the material under study in solid (voidless) form. This is furnished by a curve or relation giving the Hugoniot of the solid and a relation for computing the Gruneisen parameter, $\Gamma(v)$. Because of the lack of data, we have had to assume that the Gruneisen parameter is a constant in our computations.

The relation between the solid Hugoniot and the porous Hugoniot is derived as follows[5]. The Gruneisen equation of state is written as

$$P_f - P_s = (\Gamma/v)\ (E_f - E_s) \tag{1}$$

where P is the pressure, v is the specific volume, E is the specific internal energy, and the subscripts f and s refer to quantities in the porous and solid material respectively at the same volume v. Because the shear strengths of explosives are not known, we use the pressure to approximate the principal stress in the direction of shock propagation. The Rankine-Hugoniot energy equations for both materials are

$$E_f - E_{of} = P_f(v_{of} - v)/2 \tag{2}$$

$$E_s - E_{os} = P_s(v_{os} - v)/2 \tag{3}$$

where the added subscript, o, refers to the initial, or zero pressure, state of the material. The assumption is made that $E_{of} = E_{os}$; Boade[5] and others[8] justify this assumption on the basis that the two energies differ only by the additional small amount of surface energy in the porous material. With this assumption and substitution of equations (2) and (3) into equation (1), we obtain

$$P_f = P_s \left| \frac{v_{os} - v - 2v/\Gamma}{v_{of} - v - 2v/\Gamma} \right| \tag{4}$$

For some materials, the relation between the shock velocity, U, and the particle velocity, u, is linear, i.e.,

$$U = c_o + S\ u, \tag{5}$$

where c_o is the sound speed at zero pressure and S is the slope of the U,u curve. For such materials, a convenient representation for P_s can be derived by using the Rankine-Hugoniot equations

$$P - P_o = u\ U\ /\ v_o \tag{6}$$

and

$$U - u_o = (U - u)\ v_o/\ v. \tag{7}$$

Solving for the pressure, there results

$$P_s = \frac{c_o^2 \ (v_{os} - v)}{[v_{os} - S(v_{os} - v)]^2} \ . \qquad (8)$$

P_o (1 bar) is considered negligible compared to P in Eq. (6) and u_o in Eq. (7) is zero in applications considered here. With these approximations, equations (4) and (8) will yield the Hugoniot for the porous material.

Equations (4) and (8) are included in a computer code written by Herrmann[7]. (Also included is a method for calculating the behavior of porous materials while the pores are collapsing -- the crushup process. This method is generally known as the P-α model where α is a parameter which describes the compaction process. The required data for this code are: the Hugoniot of the solid material, a value for $\Gamma(v)$ (we assume that Γ is a constant in this report), the specific volume of the porous material, the crushup pressure (P_c), and the pressure at the elastic limit for the porous material). A computer code is described in Appendix A which solves Eqs. (4) and (8), i.e., it does not treat the compaction process.

Throughout this report we will be exploiting only a small portion of the work published by Herrmann[7]. As noted above, we do not use his scheme for calculating the pressure in the crushup region. Neither do we use his more complicated relations for describing the Hugoniot of the solid material. These latter relations remove the restrictions of linearity of the relationship between shock and particle velocities.

Although the above treatment seems to be the currently most successful treatment of granular materials, other methods of determining the Hugoniot are also used. In particular, the Russian literature on explosives frequently cites Voskobinikov et al[9]. Starting with a generalized Hugoniot for organic liquids, these workers derived an expression for an organic liquid containing bubbles. They considered it applicable to porous solids as well. Their final expression is

$$\left(\frac{u_f}{u_s}\right)^2 = 1 + \frac{2P}{(\gamma+1)\ u_s^2} \quad (v_{of}^* - v_{os}) \qquad (9)$$

where $\gamma = (C_p/C_v)$ for air and v_{of}^* is given by

$$v_{or}^* = v_{of} + \delta \frac{\gamma-1}{\gamma+1} v_{oair} \qquad (10)$$

where δ is the mass fraction of the air in the porous material.

In a recently translated article, Dremin, Shvedov, and Avdonin[10] use a more involved method for calculating the Hugoniots of porous materials. The method is described in some detail by Al'tshuler et al

in a paper[11] published in Russia in 1958. Zel'dovich and Raizer[12] also describe the method. The method starts with the use of the caloric equation of state

$$P + \frac{dE_c}{dv} = \Gamma(E - E_c)/v \qquad (11)$$

where the subscript c refers to the 0°K isotherm. This is the chief difference between this method and the one used by Herrmann and others who used the Hugoniot of the solid as the reference thermodynamic path. Equation (11) is specialized to describe a Hugoniot by replacing E by $0.5\ P(v_o - v)$, the change in energy across a shock. There results

$$v \frac{dE_c}{dv} + \Gamma E_c = \frac{\Gamma P_H}{2} (v_o - v - 2v/\Gamma). \qquad (12)$$

The subscript H means that the pressure is evaluated along the Hugoniot curve. Al'tshuler et al show how Eq. (12) can be converted into an integral equation which can be solved numerically. The reason for doing this is that E_c is a function of the volume, which has, so far, not been specified. In order to solve the equation, the function $P_H(v)$ must be known, usually from experiments. If the variable Γ is also treated as a function of the volume, it also must be specified. Dremin et al treated Γ as a constant, as will be done throughout this discussion.

Once $E_c(v)$ is known, the Hugoniot of the same material in porous form can be obtained from Eq. (12). That is,

$$P_H(v_{of},v) = \left(\frac{2v}{\Gamma} \frac{dE_c}{dv} + 2E_c \right)/(v_{of} - v - 2v/\Gamma), \qquad (13)$$

where v_{of} is the initial specific volume of the porous material. This comes about because in the derivation of Eq. (12), no assumption was made as to whether the material was continuous or discontinuous. As in the derivation of Eq. (4), it is assumed here that the surface energy of the porous material can be neglected.

Because $E_c(v)$ is known as a function of v, Eq. (13) can also be solved numerically, giving $P_H(v_{of},v)$ as a function of v for any specified value of v_{of}. This Dremin, Shvedov, and Avdonin[10] have done for RDX (1.0 g/cc), tetryl (0.86 g/cc), PETN (0.82 g/cc) and ammonium nitrate (0.86 g/cc). Their results agree well with their experimental data as is shown in a later section of this report. We used the simpler model, Eqs. (4) and (8), to compute Hugoniots for the same explosives. These results will be discussed in a later section.

In concluding this section of the report, we must point out that the above treatments of shock compression of porous materials neglects what is called the "crushup" process. This is the process which closes the voids in the porous media. Herrmann has extended his work to compute flow variables during crushup. We do not use that part of

his work because we lack the necessary input data. Required data are the sound speed in the porous material, its elastic limit, and the pressure at which it becomes void free. More elaborate models of the crushup process are available, which, because they require even more data, cannot at present, be applied to our work. As for the work of Dremin et al, they warn about extrapolating their data to pressures below 10 kbar because of the possibility of splitting of the shock waves. Hence, they are aware of the phenomena of crushup. Based on the translated articles we have seen, they do not have a computational model which accounts for the crushup process. In one Russian article, it is stated: "There is still no reliable description of the behavior of a porous material dynamically compressed to a density less than the density of the single crystal."[13]

In the next section of this report, the experimental method used to obtain Hugoniot data for 0.98 g/cc TNT is described. In a later section, the experimental data are compared with results computed using some of the models described above.

EXPERIMENTAL

The experimental configuration used in this work is shown in Figure 1. The pentolite booster and polymethyl methacrylate (PMMA) cylinder constitute the pressure-donor and pressure-attenuator parts, respectively, of the NAVSURWPNCEN Large Scale Gap Test (LSGT)[2,3]. The 50/50 pentolite booster consists of two pellets, 50.8 mm diameter by 25.4 mm long, at a density of 1.56 g/cc. The PMMA cylinder is 50.8 mm diameter and is machined to the desired length, x.

The electromagnetic velocity (EMV) gage consists of a rectangular loop of aluminum foil 0.025 mm thick and ~2 mm wide; the effective gage base length[14] used in this work was 1.11 cm. The EMV gage used in this work is in the radial configuration (i. e., the leads come out the side of the charge) because this configuration facilitates the assembly of the setup. The EMV gage is mounted on the surface of the PMMA cylinder with chloroform and the TNT is then hand pressed to the desired density of 0.98 ± 0.03 g/cc. The TNT (Lot X517) is a coarse, granular material and has an average particle size of approximately 400μ. This particle size was estimated by a partial sieve analysis.

The experimental assembly is placed in a magnetic field of ~400 gauss. This field is generated by a pair of Helmholtz coils which have a 35.5 cm diameter and 750 turns/coil of #14 wire. The coils are energized by a 20 amp, 120 volt constant current supply. The instrumentation and data reduction method used in this work are described in Reference (4).

The pressure-donor and pressure-attenuator part of the LSGT was chosen for this work because the LSGT is a calibrated pressure vs distance (P,x) and particle velocity vs distance (u,x) system which can be used with Helmholtz coils without destroying them. The main

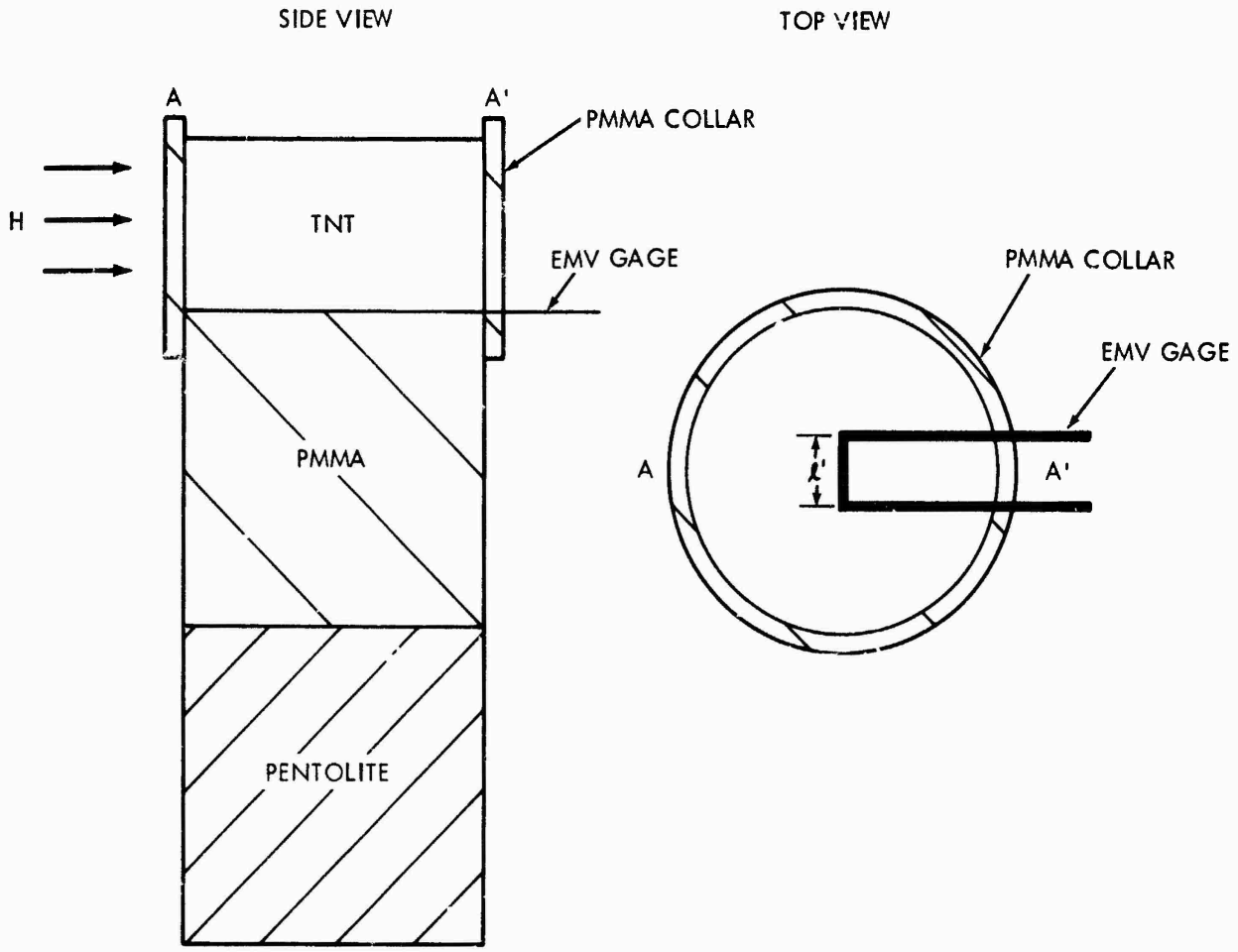

FIG. 1 EXPERIMENTAL ARRANGEMENT

drawbacks of this system are: (1) the shock front in the PMMA is curved, and (2) PMMA is a viscoelastic solid. Earlier work with the EMV gage[4] in curved shock fronts showed that the main effect of the curved fronts was to lengthen the rise time of the output signals.

ANALYSIS OF DATA

Electromagnetic Velocity Gage Technique

The EMV gage record yields a particle velocity vs time profile of the shock loaded TNT at the PMMA/TNT interface. The governing equation for this method is

$$u(t) = V(t)/(H\ \ell'\ 10^{-4}) \qquad (14)$$

where u(t) is the particle velocity as a function of time in mm/μsec, V(t) is the output voltage as a function of time in volts, H is the magnetic field in gauss, and ℓ' is the effective gage base length[14] in mm. For the radial configuration, ℓ' is the distance between the middle of the leads, see Figure 1.

The u,t data are fitted, for most cases, to a straight line by least squares using the data from the peak recorded value of u to a point 0.5 μsec beyond this value. This is the same approach as was used in Reference 3. The velocity intercept, u_e, is then assumed to be the particle velocity at the shock front. For the lowest pressure, the u,t curve had a long risetime (~500 ns) and did not have a sharp peak. For this record, we simply use the peak of the observed curve for the shock induced particle velocity.

The risetime of the u,t profiles in the porous TNT is longer than that obtained in a voidless solid by a factor of two or more. This is apparently due to the time-dependent collapse of the pores[15].

Experiments are performed using attenuators of different length so that we have several pairs of values of u_e and x, the length of the PMMA attenuator. From these data, and the known Hugoniot of PMMA we can obtain the pressure, P_e, at the interface. The process for doing this is discussed in the section "Impedance Matching".

Effects of Reaction on Gage Output

Reaction is always a potential problem in the experimental determination of the unreacted Hugoniot of a shock sensitive material. In this study, the experimental problem created by reaction is that explosives, and especially TNT, become electrically conductive and affect the gage output. The TNT is going to react to some degree, during the 0.5μsec observation time, especially at high pressures. However, even if the TNT starts to react, the initial value of the particle velocity at the interface should lie on the unreacted Hugoniot. The reason for this is the following. The shock emerging from the PMMA is non-reactive. Any reaction which occurs at the interface,

where the gage is located, must start at zero reaction and follow some type of rate law. Thus the initial shock state, and the particle velocity associated with this state, must be on the unreacted Hugoniot. The problem is to obtain this initial value without interference from reaction.

Before this problem can be solved, some idea of how reaction affects the gage is necessary. The EMV gage has been used in a non-reactive material, PMMA, in an earlier study[3]. Figure 2 is a typical gage record when the gage is located in PMMA at a distance, x = 25 mm, from the booster. Notice the fairly smooth falloff of particle velocity with time. Since PMMA is the inert used in this work the particle velocity vs time profile recorded at the PMMA/TNT interface should resemble Figure 2 if the TNT reaction does not affect the gage output. In order to see how reaction affects the gage output, an EMV gage was placed in the TNT at a position where the TNT was reacting. Figure 3 shows the results. The electrical conductivity associated with the reaction products of the TNT apparently shorts out the gage leads and causes the output of the gage to decrease rapidly. The initial particle velocity, which is the velocity at time t = 0, is the quantity of interest. To obtain this velocity, the u,t profiles must be extrapolated back to t = 0. The extrapolated value using a u,t profile similar to Figure 2 is more reliable than the value obtained using a u,t profile similar to Figure 3. If the gage leads can be adequately insulated, the u,t profiles obtained from the EMV gage at the PMMA/TNT interface should resemble the u,t profile of Figure 2.

To circumvent the problem of conductivity, especially at high pressures, it was decided to cover the EMV gage leads with an insulator. A thin (0.001 in.) layer of mica was used. A shot was fired with two gages at the interface, (where x = 12.7 mm, the length of the PMMA attenuator) one with leads covered with mica, the other bare. Figure 4 shows the resulting u,t profiles. The lower curve is the bare gage result. It is very similar to the record from the gage located in the reacting TNT, see Figure 3. The t = 0 value of the particle velocity obtained using this curve would not be very reliable. The upper curve is the mica covered gage result. This curve is very similar to the u,t profile in PMMA, see Figure 2. Thus, covering the gage leads with an insulator (mica) prevents conductivity from affecting the gage output up to at least 55 kbar which was the highest pressure used in this study.

Impedance Matching

When a shock encounters an interface between materials having different shock impedances, a shock is transmitted across the interface, and a wave is reflected back into the originally shocked material. Here impedance means the product of the density and the shock velocity. The reflected wave will be a rarefaction if the impedance of the second material is less than that of the first. Otherwise, it will be a shock wave. Solving for the strengths of the reflected and transmitted wave can be done graphically, or analytically, and is called impedance matching (or mirror image) technique.

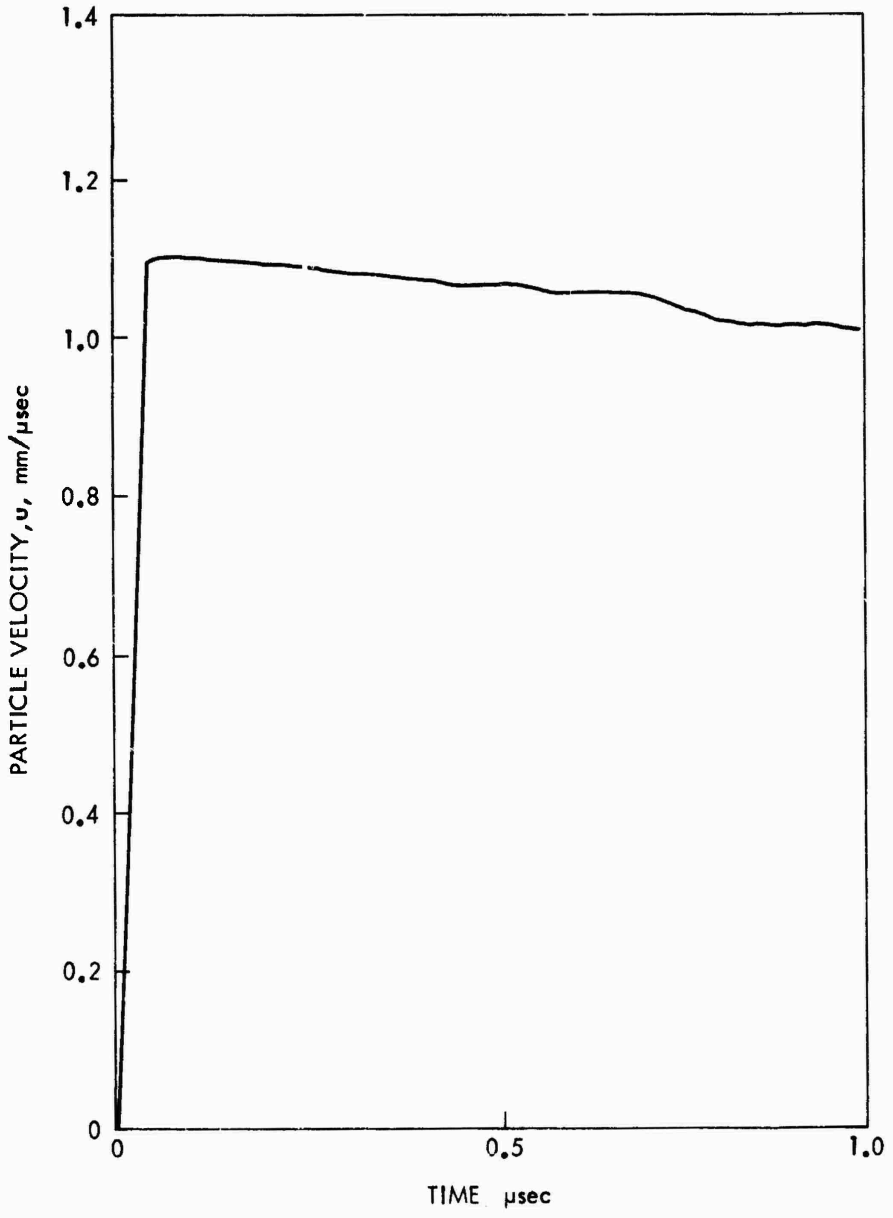

FIG. 2 u,t PROFILE IN PMMA (#271, x = 25 mm, REF. 3)

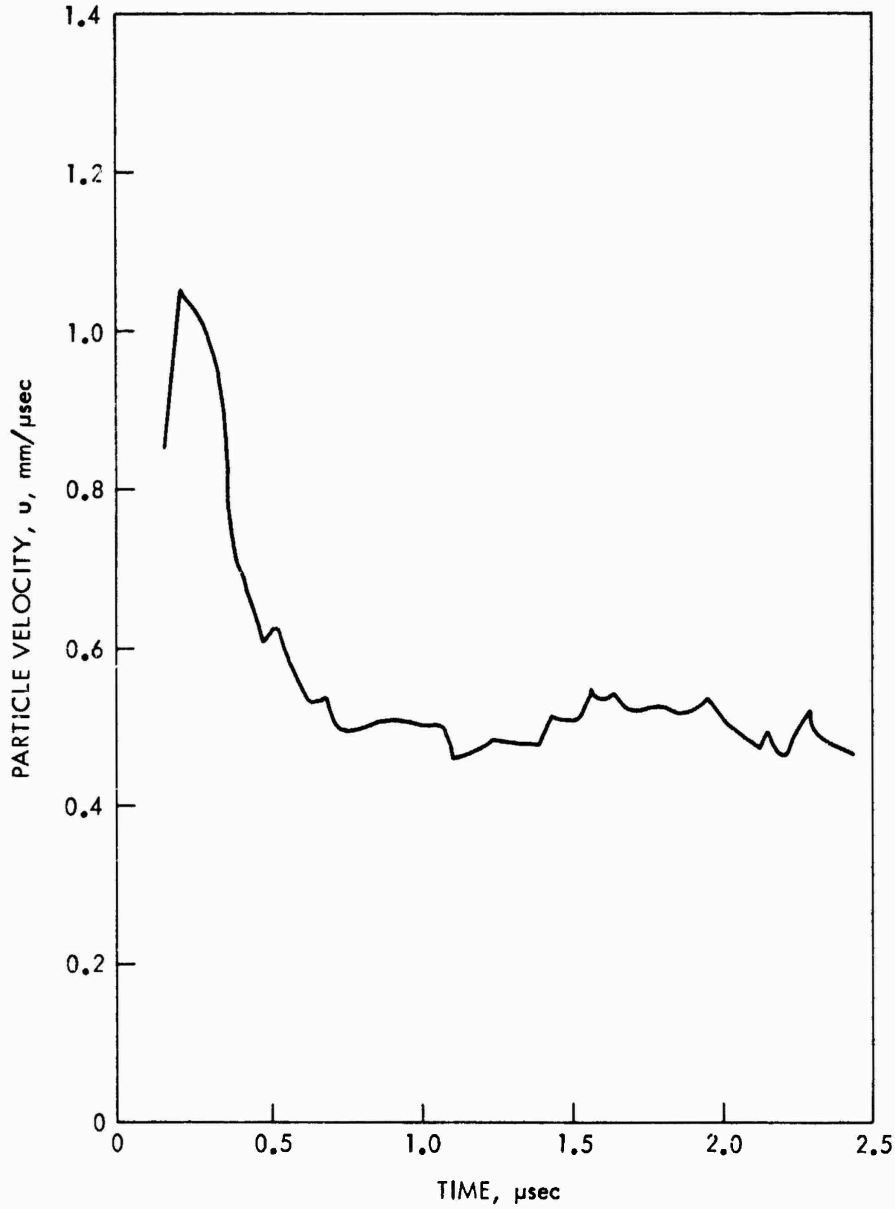

FIG. 3 u,t PROFILE IN REACTING TNT (#281B, 20.4 mm FROM PMMA/TNT INTERFACE, SEE APPENDIX E)

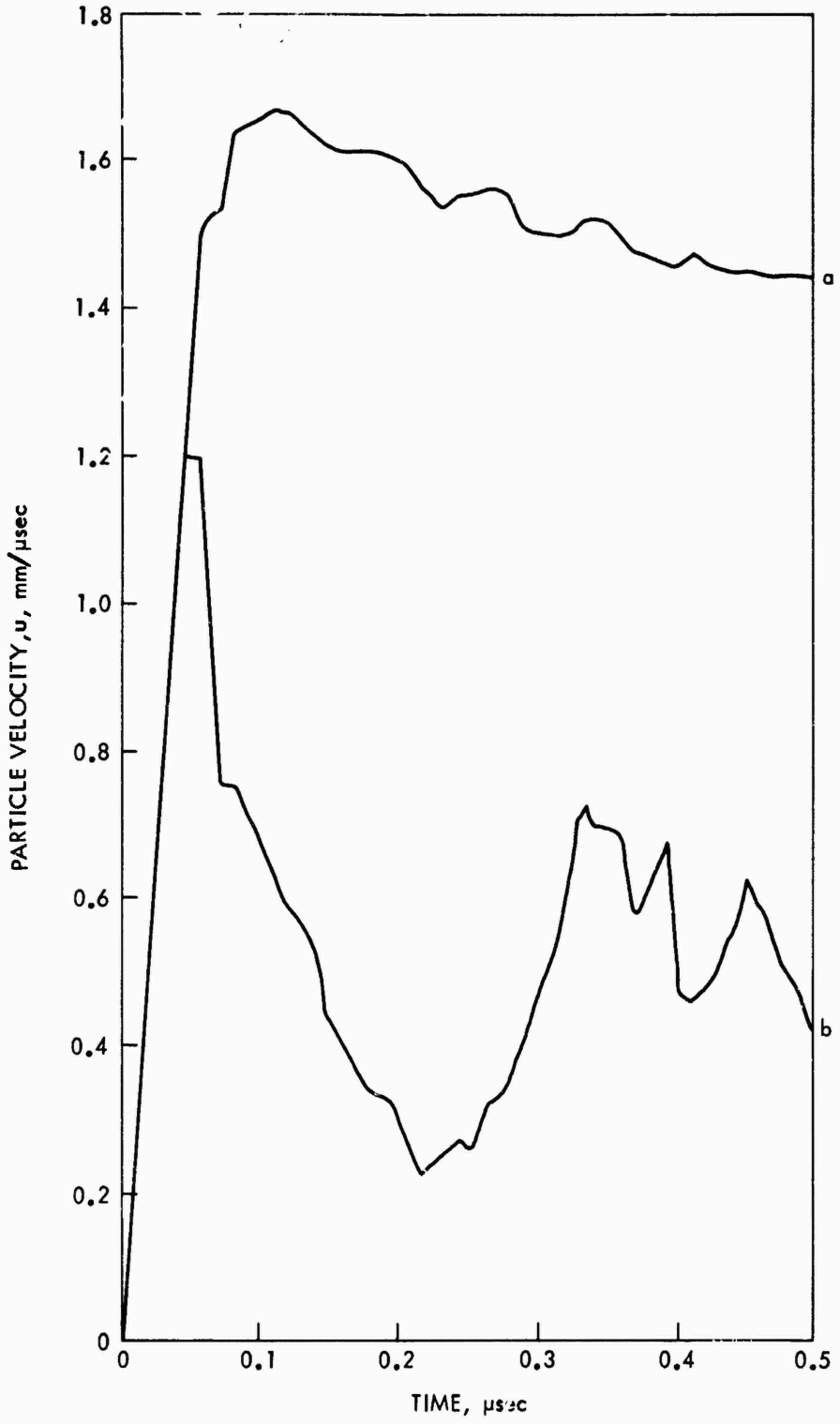

FIG. 4 u,t PROFILES FROM MICA COVERED (a) AND BARE (b) EMV GAGES AT PMMA/TNT INTERFACE (#330, x = 12.7 mm)

We have the Hugoniot curve, i.e., a relation between P and u, for PMMA for forward facing shocks. This was derived from the relations[3]

$$U = 2.561 + 1.595u \qquad u \geq 0.536,$$

and

$$U = 2.7228 + 4.0667u - 10.9051u^2 + 10.691u^3, \qquad u < 0.536, \tag{15}$$

where U and u are the shock velocity and particle velocity, respectively in mm/μsec. Substituting equation (15) into equation (6) with P_o assumed to be zero leads to

$$P = 10\rho_o(2.561u + 1.595u^2) \qquad u \geq 0.536,$$

and

$$P = 10\rho_o(2.7228u + 4.0667u^2 - 10.9051u^3 + 10.691u^4), \qquad u < 0.536, \tag{16}$$

where P is in kbars and ρ_o is the density of the PMMA, which is 1.185 g/cc. Equations (16) are represented by the curve labeled 1 in Figure 5 which represents only the first quadrant of the P,u diagram. This curve is for the case of shocks which are propagating in the forward, or +x, direction in a conventional t,x diagram. Had the shocks been backward facing, i.e., propagating into PMMA in the -x direction, the curve would pass through the origin of Figure 5 with negative slope, i.e., it would lie in the second quadrant of the P,u diagram. Such a curve can be translated to the right, see the curve labeled 2 in Figure 5. This is the P,u curve for backward facing shocks in PMMA which had a particle velocity of $2u_1$ in the forward direction prior to being shocked. Curve 2 is said to be the reflection of curve 1 about the line $u = u_1$. Mathematically, any such curve is described by replacing u in equation (16) by $(2u_1-u)$.

As noted above, the wave reflected back into the PMMA may be a shock or a rarefaction. If it is a shock, values of P and u induced by it will lie on the part of curve 2 above the intersection, point A in Figure 5. This part of curve 2 is exact for reflected shocks. If the reflected wave is a rarefaction, we use the part of curve 2 which lies below point A. But flow variables in a relief wave (simple wave) are governed by adiabatic or isentropic relations. Curve 2 is exact only for shock compression, a process which produces entropy. To solve for a relief wave in the PMMA, the curves should be those for an adiabatic process.

A common approximation is made by noting that the transition through a simple wave gives values of the flow variables which agree to second order with those produced by a weak shock[16]. So to second order, the segment of curve 2 below point A of Figure 5, and segments

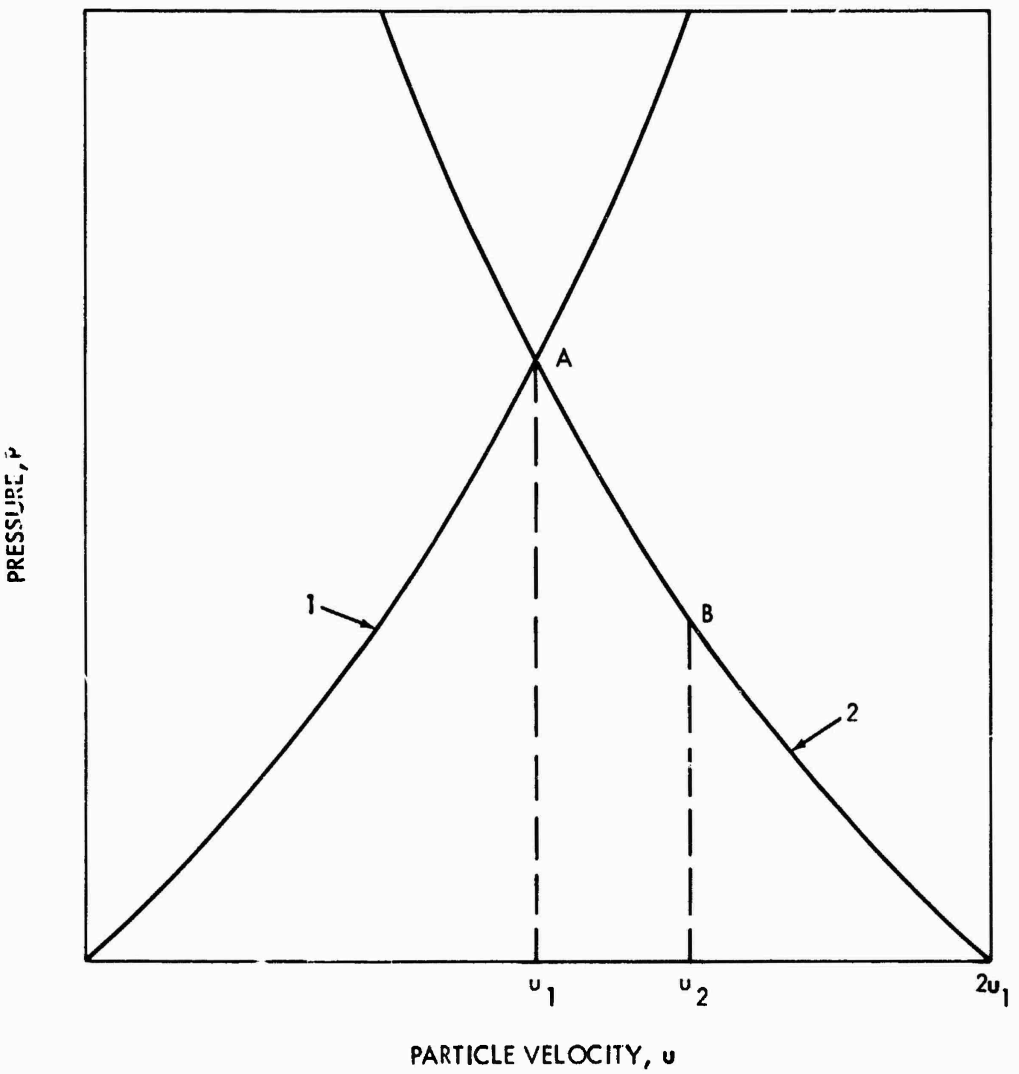

FIG. 5 IMPEDANCE MATCHING DIAGRAM

of similar curves, can be used to approximate the relation between P and u in a simple relief wave. These curves are generally referred to as 'cross curves' and a curve can be drawn by specifying either P or u on the Hugoniot, curve 1.

In a previous section, pairs of values of x and u_e were obtained from the experimental records. Because the LSGT calibration[3] gives u as a function of x, measuring the length of the PMMA attentuator yields the particle velocity, u_1, at the PMMA/TNT interface just before the shock enters the TNT. The LSGT calibration is, for a 50/50 pentolite donor (1.56 g/cc),

$$u_1 = 1.7735 \exp(-0.01841\ x) + 0.8765 \exp(-0.3495\ x) \qquad x \leq 36 \text{ mm}$$

$$u_1 = 0.0905 + 4.0877 \exp(-0.04451\ x) \qquad x > 36 \text{ mm} \qquad (17)$$

where u_1 is in mm/μsec. The pressure associated with u_1 is obtained from equation (16) and is designated P_1. The particle velocity in the TNT, designated u_e, is obtained from the experimental records as described in the section "Electromagnetic Velocity Gage Techniques". There results a set of values of u_1, P_1, and u_e for each experiment. It remains to determine the value of P_e, the pressure actually transmitted into the TNT.

For each set of data, the PMMA cross curve (such as curve 2 in Figure 5) is drawn so that it crosses curve 1 at $u = u_1$. Then the line $u = u_e$ is drawn and the value of the pressure where this line intersects the cross curve is read. This pressure is the value of the transmitted pressure, P_e. This process is repeated for each set of values of u_1, P_1, and u_e.

Viscoelastic Effects in PMMA

In the previous section, the PMMA was assumed to behave in a simple way when it expanded from a shocked state. Rate effects, elastoplastic and viscoelastic effects, and the effects due to the increase of entropy behind the shock wave were neglected. Data on the way PMMA behaves as it is relieved from the shocked state are scarce. From the work of Schuler and Nunziato[17] and Barker and Hollenbach[18], all of Sandia Laboratories, it is inferred that PMMA is a nonlinear, viscoelastic material. The data leading to this inferrence was obtained from observing shocked samples of PMMA with laser interferometry. These data show that the reflected Hugoniot as discussed in the previous section is only an approximation to the observed release path. In References (17) and (18), the observed data were converted to stress and strain. In the stress vs strain diagram, the unloading curve lies below the loading (shock Hugoniot) curves. A knowledge of how these experimentally based data appear in the pressure-particle velocity plane is needed for the present work.

Unfortunately, References (17) and (18) do not give values of the particle velocity for each value of the strain (although particle velocity was the variable measured in the experiments).

The data of References (17) and (18), however, can be used to obtain values of the particle velocity by using the relation

$$du = c \frac{d\rho}{\rho} \quad , \tag{18}$$

which relates the change in the particle velocity, u, to a change in the density, ρ, across an increment of a simple wave. The variable c is the local sound speed. Engineering strain, ε, was used in References (17) and (18), so that

$$d\varepsilon = \frac{\rho_o}{\rho} \frac{d\rho}{\rho} \quad . \tag{19}$$

Combining quations (18) and (19) yields

$$u = \int \frac{c\rho}{\rho_o} d\varepsilon \quad . \tag{20}$$

The quantity c is obtained from

$$c^2 = \frac{dP}{d\rho} = \frac{dP}{d\varepsilon} \frac{d\varepsilon}{d\rho} \quad , \tag{21}$$

where $d\varepsilon/d\rho$ is obtained from equation (19) to give

$$c^2 = \frac{dP}{d\varepsilon} \frac{\rho_o}{\rho^2} \quad . \tag{22}$$

Combining Equation (20) and (22) gives

$$u = \rho_o^{-\frac{1}{2}} \int \left(\frac{dP}{d\varepsilon}\right)^{\frac{1}{2}} d\varepsilon \quad . \tag{23}$$

Sets of data from References (17) and (18) were fitted to a cubic by the method of least squares, giving P as a function of ε, i.e.,

$$P = A + B\varepsilon + C\varepsilon^2 + D\varepsilon^3 \quad . \tag{24}$$

Differentiating Equation (24) and substituting for $dP/d\varepsilon$ in equation (23) gives an integrand which can be handled analytically. There results

$$u = \rho_o^{-\frac{1}{2}} \left[\frac{(3D\varepsilon + C)}{6D} R + \frac{(3BD - C^2)}{6D} \left\{ (3D)^{-\frac{1}{2}} \log[6D\varepsilon + 2C + R\sqrt{12D}] \right\} \right] + \text{constant} \tag{25}$$

where $R = (B + 2C\varepsilon + 3D\varepsilon^2)^{\frac{1}{2}}$. The constant is evaluated by noting that the material is relieved from a state located on the Hugoniot for which $\varepsilon = \varepsilon_1$ and $u = u_1$. Equation (25) is for a forward facing wave, so the cross curve is obtained from

$$u_c = 2u_1 - u. \tag{26}$$

We now have relations between P and ε from the cubics fitted to the data of references (17) and (18), and between u_c and ε, by equations (25) and (26). Several of the cross curves are plotted in Figure 6 along with the mirror image of the Hugoniots. The numbers at the upper ends of each curve give the pressure in kilobars where the curve intersects the Hugoniot curve for forward facing shocks. That is, these are the shock pressures from which the PMMA expands. For 8.36, 11.99, and 18.34 kbar, there is no significant difference between the curves as calculated and the reflected Hugoniots. For 29.7 kbar, the calculated curve lies below the reflected Hugoniot by about one or two kilobars over the range of pressures of 8 to 22 kbar. Hence, the values of P_e obtained by impedance matching should be reduced by about 2 kilobars. Even though Schuler and Nunziato[17] have investigated PMMA up to a pressure of 60 kbar, no data above 29.7 kbar have been found by the authors with which further calculations could be made. Schuler and Nunziato[17] do state that viscoelastic effects become of secondary importance above ~40 kbar and below ~7 kbar. In this study, we have used the calculated curves in Figure 6 to estimated the correction due to viscoelastic effects. Between 30 and 60 kbars, the correction was estimated by assuming that the viscoelastic effect is symmetric about 30 kbar. Thus the correction becomes progressively smaller from 30 to 60 kbar.

Note that two of the calculated curves in Figure 6 are terminated before P = 0. This was done because the data of references (17) and (18) also terminated at these pressures. Extending these curves would require extrapolating the cubic fit of P vs ε to P = 0.

Data

Most of the raw data obtained in this study are listed in Table 1. Three shots in the pressure range 18-44 kbar showed some evidence of reaction of the explosive and are not included. The P_e data of Table 1 were obtained using the reflected PMMA Hugoniot. As is evident from Table 1, there is some scatter in density of the individual shots. Using the computer code developed by Hermann[7] (see Appendix A) to predict the Hugoniots of porous materials, the data of Table 1 were adjusted to the single density of 0.98 g/cc. This was accomplished as follows. Calculated Hugoniots for TNT at 0.95, 0.96, 0.97, 0.98, and 1.01 g/cc were generated and plotted. Then for each experiment, the distance between the calculated TNT Hugoniot at the density of the experiment and the calculated TNT Hugoniot at 0.98 g/cc along the reflected PMMA Hugoniot was determined. The experimental datum point was then moved this distance along the reflected PMMA Hugoniot. This correction for density results in new values for both u and P for the TNT data. These results are listed in Table 2 and plotted as open

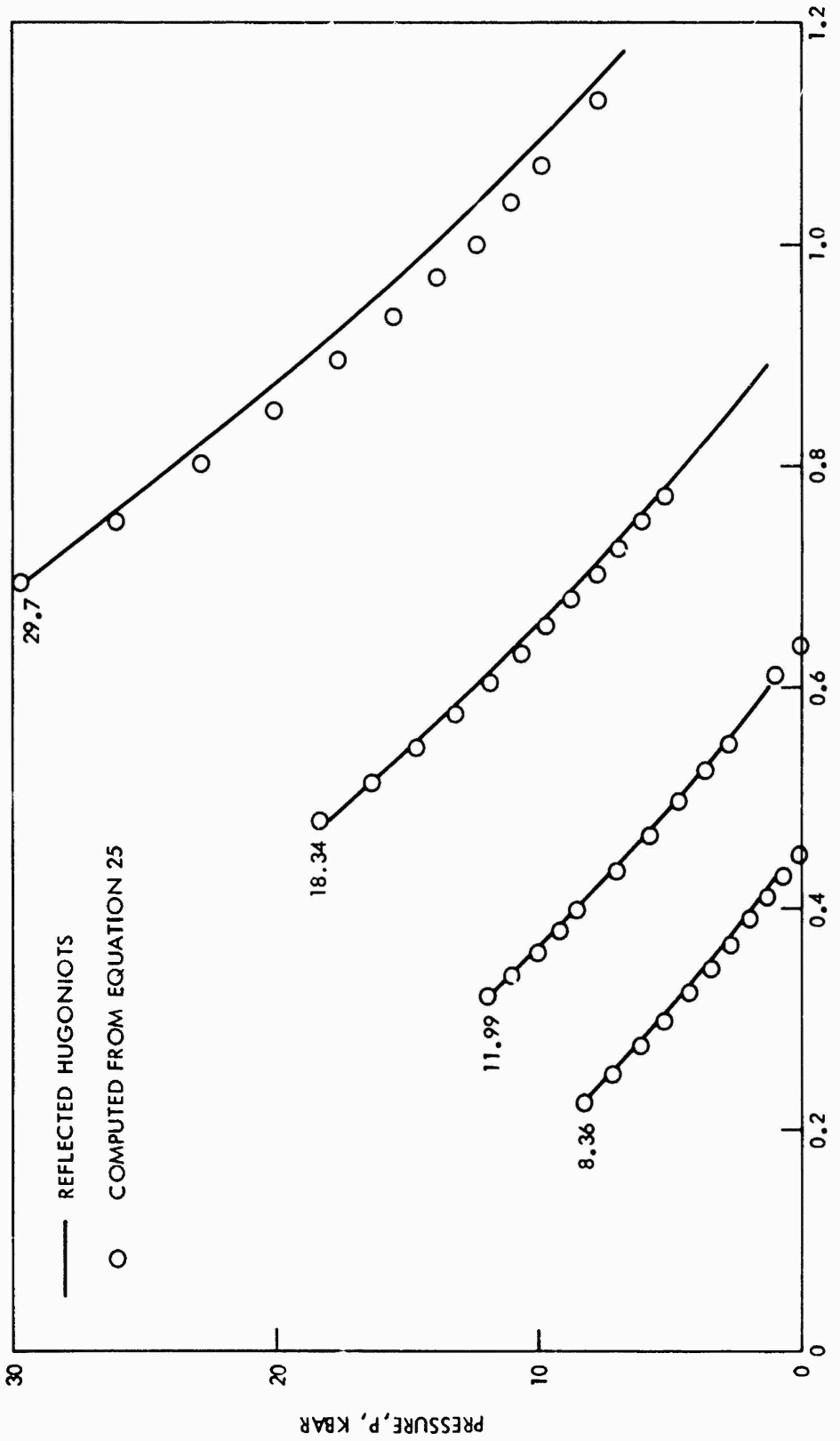

FIG. 6 PRESSURE, PARTICLE VELOCITY RELEASE CURVES FOR PMMA

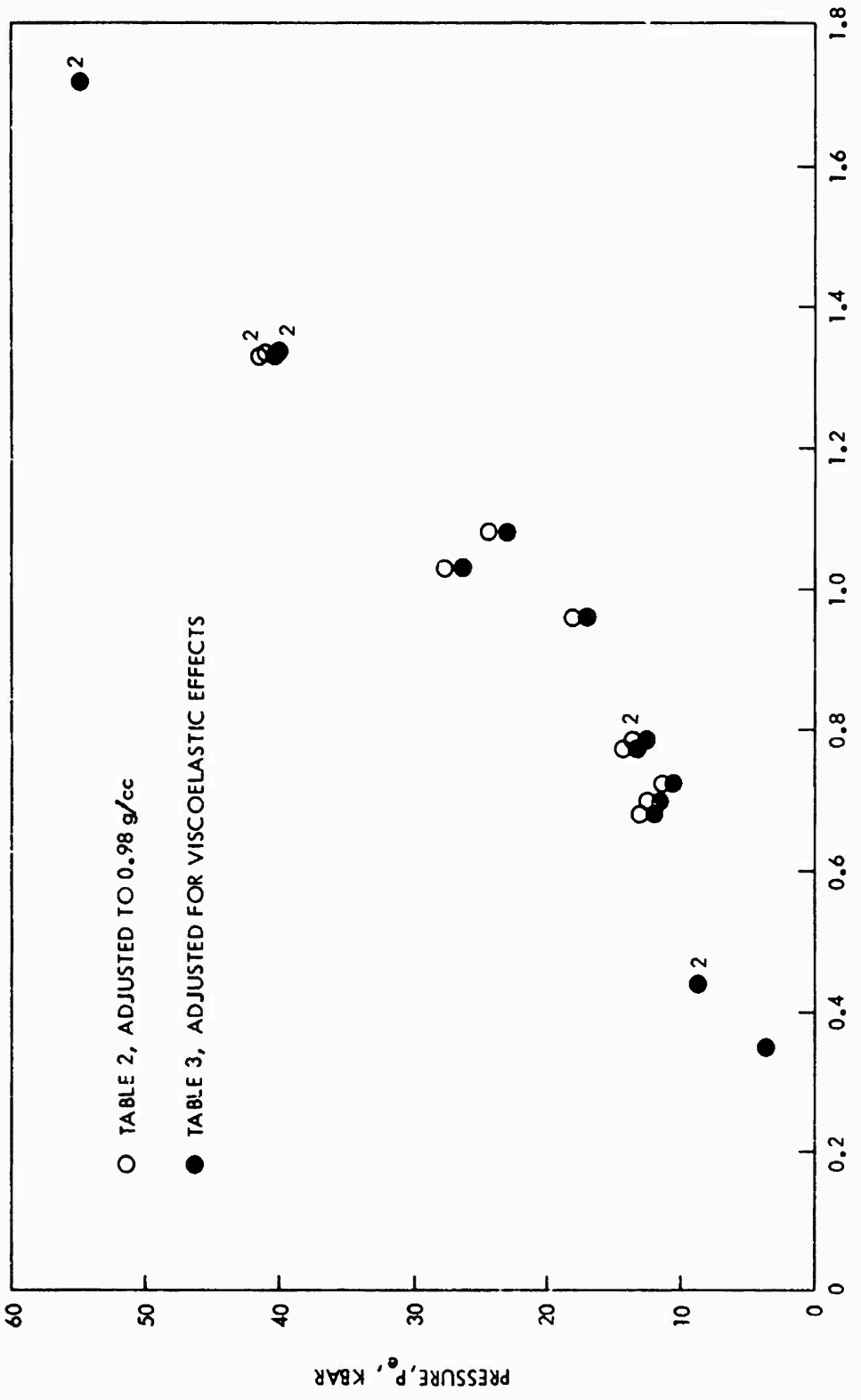

FIG. 7 HUGONIOT DATA FOR POROUS TNT, $\rho_o = 0.98$ g/cc

TABLE 1

HUGONIOT DATA FOR POROUS TNT
(Mirror Image Approximation)

u_e mm/μsec	P_e Kbar	ρ_o g/cc	Length of PMMA mm	u_1 mm/μsec	P_1 Kbar	Shot No.
0.350[a]	3.6	0.96	76.2	0.228	8.7	254
0.450	8.3	0.96	63.5	0.333	12.9	257
0.440	8.6	0.97	63.5	0.333	12.9	252
0.700	12.5	0.96	50.8	0.517	20.7	285A
0.680[b]	13.0	1.01	50.8	0.517	20.7	251
0.730	11.2	0.97	50.8	0.517	20.7	253
0.772[m]	14.2	0.98	46.8	0.560	22.9	336
0.793[m]	13.7	0.98	47.7	0.578	23.8	333
0.794[m]	13.7	0.98	47.7	0.578	23.8	332
0.970	17.4	0.95	44.5	0.654	27.9	293
1.080[m]	24.5	0.98	38.2	0.837	38.6	335
1.030	27.8	0.98	38.1	0.840	38.8	290
1.300	43.0	1.01	25.4	1.111	56.9	316
1.310	42.3	1.01	25.4	1.111	56.9	291
1.340[m]	41.0	0.98	25.4	1.111	56.9	327
1.720[m]	55.0	0.98	12.7	1.413	80.4	330
1.720[m]	55.0	0.90	12.7	1.413	80.4	331

a) Peak of u,t curve.

b) 5 mil gage, all others 1 mil.

m) mica covered gage leads.

TABLE 2

HUGONIOT DATA FOR POROUS TNT ADJUSTED TO 0.98 G/CC
(Mirror Image Approximation)

0.98 g/cc			Raw Data, Table 1	
u_e mm/μsec	P_e Kbar	Shot No.	u_e mm/μsec	P_e Kbar
0.350[a]	3.6	254	0.350	3.6
0.435	8.4	257	0.450	8.3
0.440	8.6	252	0.440	8.6
0.680	13.0	285A	0.700	12.5
0.700[b]	12.5	251	0.680	13.0
0.725	11.4	253	0.730	11.2
0.772[m]	14.2	336	0.772	14.2
0.793[m]	13.7	333	0.793	13.7
0.794[m]	13.7	332	0.794	13.7
0.960	18.0	293	0.970	17.4
1.080[m]	24.5	335	1.080	24.5
1.030	27.8	290	1.030	27.8
1.330	41.5	316	1.300	43.0
1.340	41.0	291	1.310	42.3
1.340[m]	41.0	327	1.340	41.0
1.720[m]	55.0	330	1.720	55.0
1.720[m]	55.0	331	1.720	55.0

a) Peak of u,t curve.

b) 5 mil gage, all others 1 mil.

m) Mica covered gage leads.

circles in Figure 7. The changes are small except for the points at ~ 40 kbar where the correction is the largest.

The data contain five sets of replicate shots (i.e., each set has the same attenuator length). For the first set, shots 252 and 257, u_e has the values of 0.440 and 0.435 mm/μsec (see Table 2). The resultant values of P_e, 8.6 and 8.4 kbar, are within ± 1.2% of the average for this attenuator length. For the second set, shots 285A, 251, and 253, u_e = 0.680, 0.700, and 0.725 mm/μsec, respectively, with resulting P_e's of 13.0, 12.5, and 11.4 kbar. These pressures are within ± 7.3% of the average at this attenuator length. For the third set, shots 332 and 333, u_e = 0.794 and 0.793 mm/μsec, respectively, with the same value of P_e, 13.7 kbar. For the fourth set, shots 316, 291, and 327, u_e = 1.330, 1.340, and 1.340 mm/μsec, respectively, with resulting P_e's of 41.5, 41.0, and 41.0 kbar. The pressures are within ± 0.8% of the average. The final set of replicate shots, 330 and 331, have the same value of u_e, 1.720 mm/μsec, and P_e, 55.0 kbar.

Because the calculated release paths in Figure 6 do not coincide with the reflected Hugoniots, we have to repeat the impedance matching solutions which were described previously. This time we use information such as that shown in Figure 6 to draw viscoelastic release paths through each predetermined point, (u_1,P_1), i.e., points such as that labeled A in Figure 6. Each of these points lie, of course, on the Hugoniot for forward facing shocks in the PMMA and are determined solely by the length of the attenuator, see Equations 16 and 17. The amount of the offset of the new curves from the reflected Hugoniots is determined by interpolating in the data of Figure 6 and assuming that the correction is symmetrical about the release path for a 30 kbar shock. This process gives corrections which are significant for values of P_e which lie between 10 and 40 kbars, see Table 3. The maximum correction in P_e, 1.5 kbars, occurs at a value of u_e of about 1.05 mm/μsec and P_e of about 25 kbars. On a percentage basis, the maximum correction, about 9%, occurs at 0.725 mm/μsec and 11.4 kbars, see Table 3.

Data on the dynamic compressibility of 1.0 g/cc TNT has been published by two groups of Russian investigators. Vasil'ev, Bolkhovitinov, and Khrisotoforov[19] employed the EMV gage in 1.0 g/cc TNT. The P,u data obtained from their results are plotted in Figure 8 as open triangles. The results of Table 3 are plotted in Figure 8 as solid circles for comparison. The errors in pressure of our data were computed using the method described in Appendix B. The error in particle velocity lies within the size of the circles. As is evident from the figure, Vasil'ev's results diverge from ours as the pressure increases. This divergence is due to the fact that Vasil'ev's EMV gage is located inside the TNT sample and is thus affected by any reaction which has had time to build up in the TNT as the shock wave travels from the interface to the gage location. These authors are aware of this because they report that the shock velocity builds up with increasing distance in the sample. Thus, except for the very low pressure points, their data represents points on various reacted Hugoniots. Dremin, Koldunov, and Shvedov[20] have investigated the

TABLE 3

HUGONIOT DATA FOR POROUS TNT, ρ_o = 0.98 G/CC, ADJUSTED FOR ESTIMATED VISCOELASTIC EFFECTS IN PMMA

u_e mm/μsec	P_e Kbar	U mm/μsec	v cc/g	Shot No.
0.350[a]	3.6	1.05	0.680	254
0.435	8.4	1.97	0.795	257
0.440	8.6	1.99	0.795	252
0.680	12.0	1.80	0.635	265A
0.700[b]	11.5	1.68	0.594	251
0.725	10.4	1.46	0.515	253
0.772[m]	13.2	1.74	0.551	336
0.793[m]	12.7	1.63	0.525	333
0.794[m]	12.7	1.63	0.525	332
0.960	17.0	1.80	0.478	293
1.080[m]	23.0	2.17	0.513	335
1.030	26.3	2.60	0.617	290
1.330	40.5	3.11	0.583	316
1.340	40.0	3.06	0.572	291
1.340[m]	40.0	3.05	0.572	327
1.720[b]	55.0	3.26	0.428	330
1.720[m]	55.0	3.26	0.428	331

a) Peak of u,t curve.

b) 5 mil gage, all others 1 mil.

m) Mica covered gage leads.

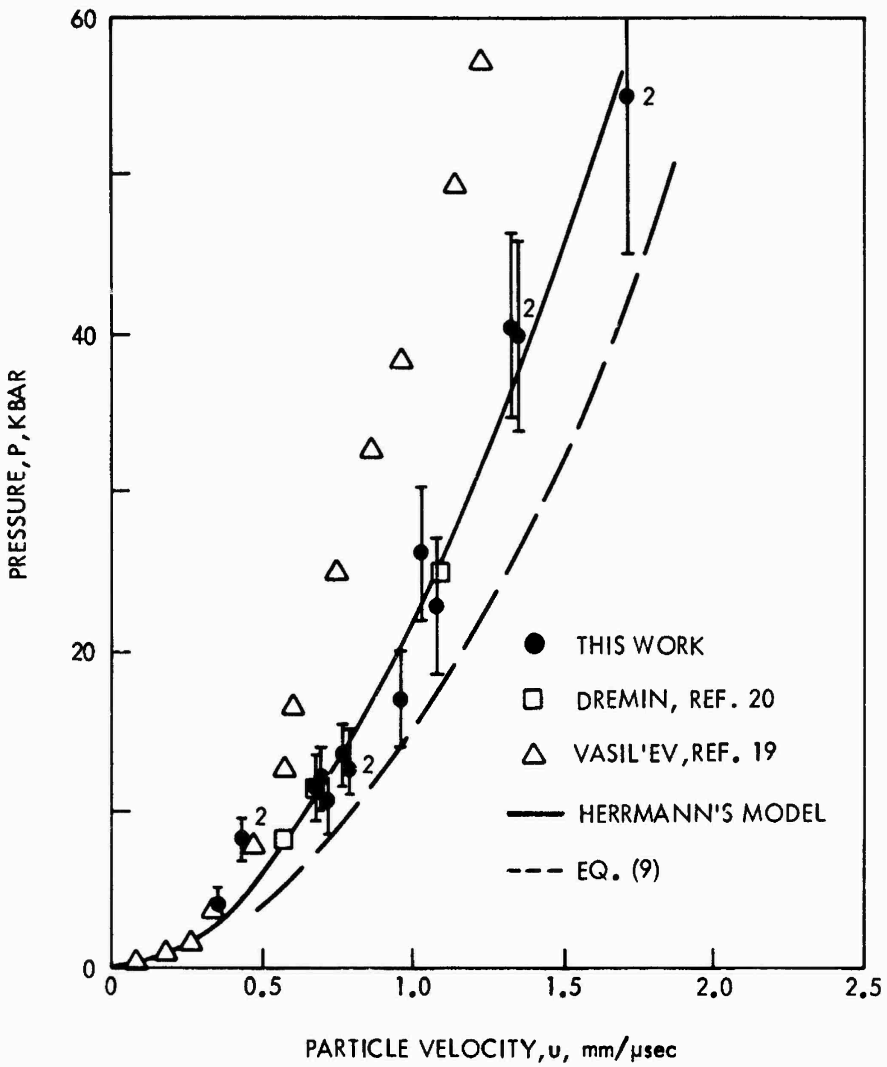

FIG. 8 COMPARISON OF DATA FOR POROUS TNT

buildup of particle velocity and shock velocity in 1.0 g/cc TNT using the EMV gage. Although most of their data were obtained from gages located in the TNT charges, Dremin et al report some results where the gage was located at the interface. Such data will lie on the unreacted Hugoniot as was discussed in the earlier section entitled "Effects of Reaction on Gage Output". These interface data, which were obtained from Figure 2 of Dremin's paper, are plotted in Figure 8 as open squares. As is evident from the figure, Dremin's data agree very well with ours.

A Hugoniot is obtained experimentally by measuring two of the following quantities: pressure, particle velocity, shock velocity, and volume. Once two of these quantities have been related to each other, the other two can be calculated using hydrodynamic relations. In this study, pressure and particle velocity were obtained experimentally. Besides the pressure - particle velocity plane, Hugoniots are frequently presented in the pressure - volume and shock velocity - particle velocity planes.

The shock velocity (U) - particle velocity (u) representation of the Hugoniot for 0.98 g/cc TNT is obtained by using u_e and P_e from Table 3 and Equation (6) with $v_o = 1/\rho_o$ and P_o assumed to be zero. The resulting shock velocity values are presented in column 3 of Table 3 and plotted as a function of u in Figure 9.

The pressure - volume (P-v) representation of the Hugoniot for 0.98 g/cc TNT is obtained by using the P_e and u_e data of Table 3 and the following equation:

$$v = v_{of} - u_e^2 / P_e \qquad (27)$$

where v_{of} is the initial volume of the TNT. The calculated values of the volume are presented in column 4 of Table 3. Figure 10 is the resulting P,v plot. The errors in P and v were obtained using Equations (B7) and (B8) of Appendix B. The large errors in volume is due to the fact that even small errors in P and u can cause a relatively large error in v.

COMPARISON OF CALCULATED AND EXPERIMENTAL HUGONIOTS FOR POROUS EXPLOSIVES, DATA FROM NAVAL SURFACE WEAPONS CENTER AND OTHER SOURCES

The experimentally determined Hugoniot for TNT at 0.98 g/cc can now be compared with the results from computational models. The required data for Herrmann's code are: the Hugoniot of the solid material, a value of $\Gamma(v)$ (or Γ_o if $\Gamma(v)$ is not available), and the specific volume of the solid. The crushup part of the code cannot be used because values of important parameters are not known, i.e., the elastic limit, the crushup pressure, and the sound speed. The Hugoniot and Γ_o for solid TNT at a density of 1.614 g/cc are[21]

$$U = 2.39 + 2.05u \qquad (28)$$

and

$$\Gamma_o = 0.737 \qquad (29)$$

where U and u are in mm/μsec. The resulting Hugoniot for unreacted

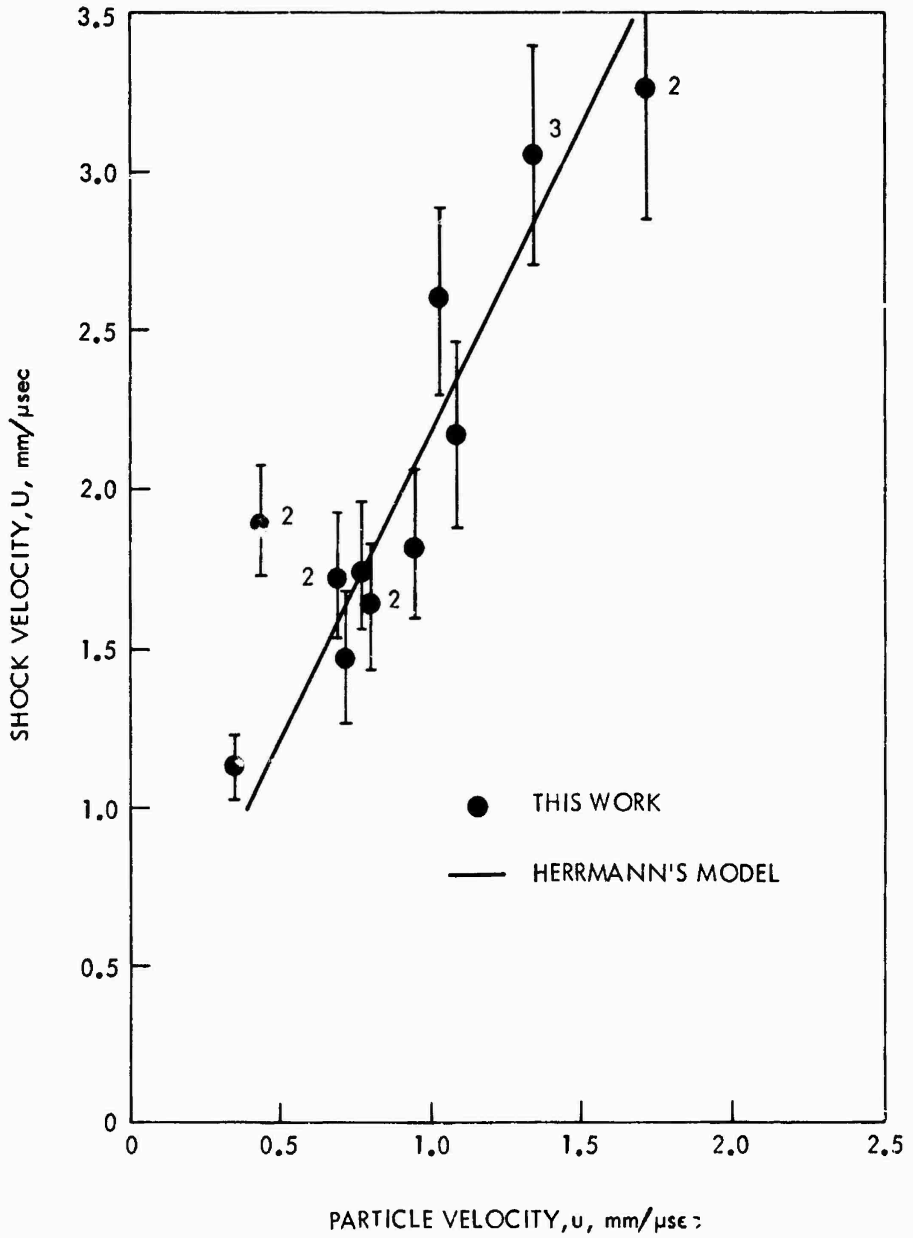

FIG. 9 U,u PLOT OF 0.98 g/cc TNT HUGONIOT

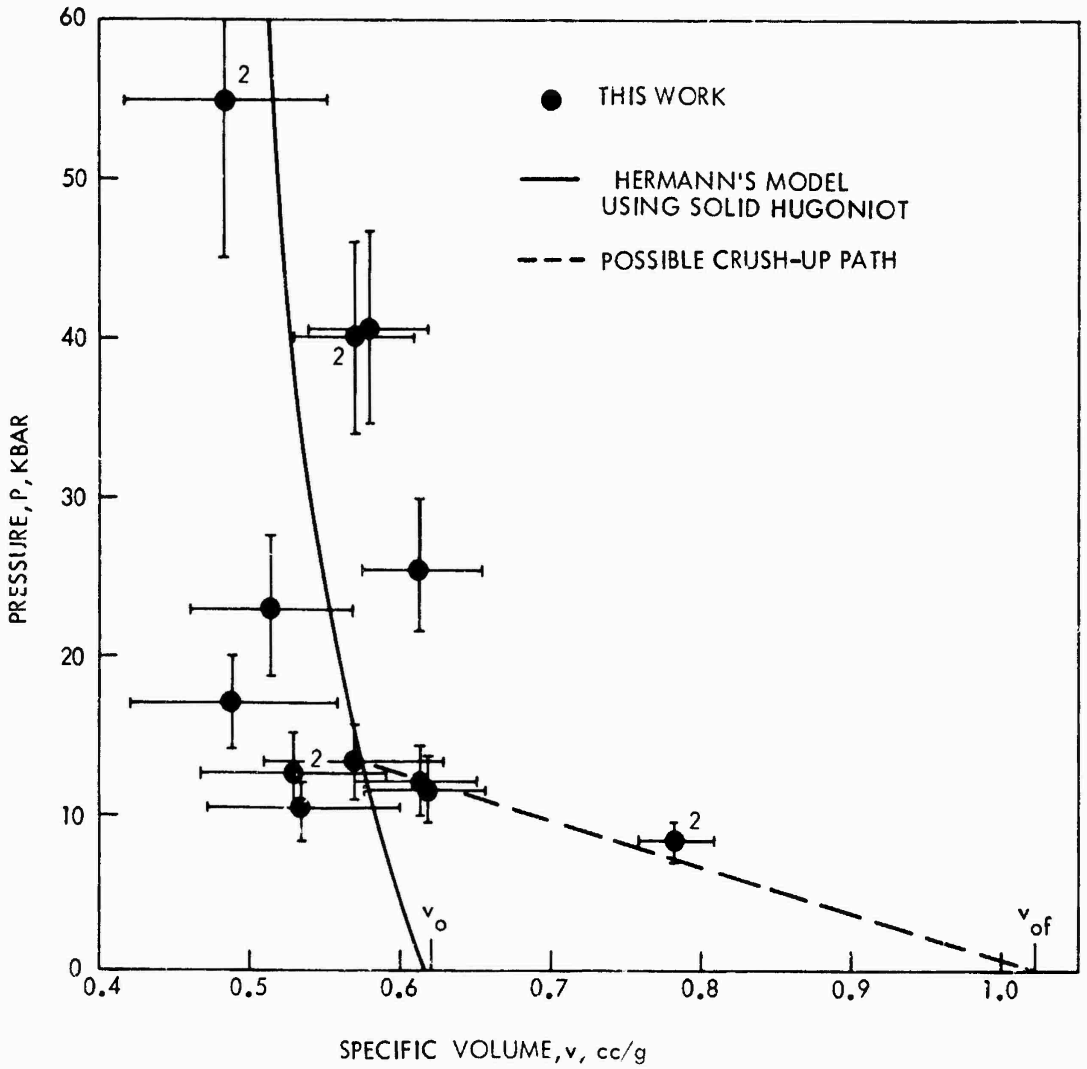

FIG. 10 P, v PLOT OF 0.98 g/cc TNT HUGONIOT

TNT at a density of 0.98 g/cc is shown as the solid curve in Figure 8 (P,u plane). Except for the two pressure points at ~ 8.5 kbar, the calculated Hugoniot agrees with the experimental data to within the calculated error in pressure and particle velocity. The data at ~ 8.5 kbar are better explained in the P-v plane and will be discussed below. Another computed Hugoniot is shown in Figure 8 as a dashed line. This is based on the theory given in Reference (9) and is expressed as Equation (9) above. It requires the use of Equations (6) and (28). The results of this model do not represent the experimental data at all well. We have not tried to readjust the values of any of the parameters in Equation (9) to get a better fit to the experimental data. The Herrmann model gives such good results with no adjustment of parameters that only a comparison of this model and the experimental results in the U,u and P,v planes will be presented in the following discussion.

The calculated Hugoniot for 0.98 g/cc TNT in the U,u plane is plotted in Figure 9 as a solid curve. Except for the two data points at u ~ 0.44 mm/μsec and U ~ 1.98 mm/μsec, the calculated Hugoniot agrees with the experimental data. As mentioned above, these two data points are more profitably discussed in the P,v plane. The experimental data (omitting the above mentioned two data points) were fitted to a straight line by the method of least squares and the resulting equation is

$$U = 0.366 + 1.813\ u \qquad (30)$$

where U and u are in mm/μsec. The calculated Hugoniot for this density is nearly a straight line. The constants for this straight line were determined by fitting the computed results to a straight line by the method of least squares. (The computed results are individual points. The number of points and the separation of the points is determined by the step size used in the computer code, see Appendix A.) The resulting equation is

$$U = 0.307 + 1.848\ u. \qquad (31)$$

The experimental result is essentially parallel to but lies 0.059 mm/μsec above the calculated Hugoniot.

In the P,v plane (Figure 10), the calculated Hugoniot is again plotted as a solid curve. The agreement between the experimental data and the calculated Hugoniot does not seem to be as good as in the P,u and U,u planes. But as was mentioned in the preceeding section, a large error in the value of v can result from small errors in P and u. Taking this fact into account, the agreement is reasonable.

The two data points at P ~ 8.5 kbar and v = 0.795 cc/g of Figure 10 correspond to the two data points in the P,u and U,u planes which did not agree with the calculated Hugoniot (Figures 8 and 9). The calculated Hugoniot, however, shown in Figures 8, 9, and 10 was obtained by neglecting, among other phenomena, the crushup process. These two data points probably lie on the crushup portion of the Hugoniot. The dashed line in Figure 10 represents a possible crushup path of the Hugoniot. It is an arbitrary straight line originating at v_{of} and ending at the calculated Hugoniot. However, there are too few data

available to properly define this portion of the Hugoniot. Another possibility which could explain the position of these two data points is that melting of the TNT may be occurring. This possibility has been investigated but no conclusion about melting could be drawn because buildup to detonation occurred too rapidly and erased any hint of a phase change. The subject of melting of the TNT is more fully discussed in Appendix C. The investigation of melting involved experimental work with 1.3 g/cc TNT which yielded some data for the unreacted state. These results are presented in Appendix D. A third possibility for the position of these two data points is that crush-up and melting could be occurring simultaneously.*

Data on five other porous explosives are available in the Russian literature from which the unreacted Hugoniots can be calculated and compared with experimental results. Densities of the porous explosives, the coefficients for the relation $U = c_o + Su$ for the solid materials and values of Γ_o for each explosive are given in Table 4. Tabulated results of the computations using the Herrmann model are listed in Table A4 of Appendix A. Some of these results are discussed below.

Data for NB-40 (60% pyroxyline, 40% nitroglycerine) are from Reference 22; the remainder are from Reference 10. Computed and experimental results are shown for NB-40 in Figure 11 as a plot of shock velocity as a function of particle velocity. The experimental results are more closely approximated by the results from Herrmann's code (solid curve) than by those from Equation (9)(the Russian approximation, dashed curve). This makes two cases in which this Russian approximation gives the worse set of results. In the following, only the Herrmann model will be used because of its demonstrated superiority.

For the other four materials listed in Table 4, results are shown in the U,u plots of Figures 12 through 15. Results shown are (a) the experimental results as reported in Reference 10, (b) results of computations as given by the same source using the values of Table 4, and (c) results computed with the Herrmann model also using the values of the parameters given in Table 4. In their computations, the Russians used the method based on the 0°K isotherm as briefly described in the section, "Computational Models". The Russians reported computed results at 25, 50, 75, 100, and 150 kbar. These data are recorded in Figures 12 through 15 as points rather than as curves.

The results for RDX are shown in Figure 12 where it is seen that the Russian computations are in no better agreement with their experimental data than are the results of Herrmann's model. Thus, it appears that the much more involved method used by the Russians is not necessary because the simpler model gives equivalent results.

For tetryl, PETN, and AN, the Russians list two values of the shock velocity for each listed particle velocity. They did this because shock velocity was determined by two different methods. Their directly measured values of shock velocity for these three materials have been plotted. Where possible, the value which they obtained by

*Data on the buildup of particle velocity in 0.98 and 1.30 g/cc TNT are presented in Appendix E.

TABLE 4

PARAMETERS FOR FIVE EXPLOSIVES FOR THE HERRMANN MODEL

Explosive	Density g/cc	C_o mm/μsec	S	Γ_o	Density of Solid g/cc	Ref.
NB-40	1.00	1.70	1.85	1.50	1.63	22
RDX	1.00	2.87	1.61	2.60	1.80	10
Tetryl	0.86	2.17	1.91	1.65	1.73	10
PETN	0.82	2.42	1.91	1.70	1.77	10
AN	0.86	2.20	1.96	0.90	1.73	10

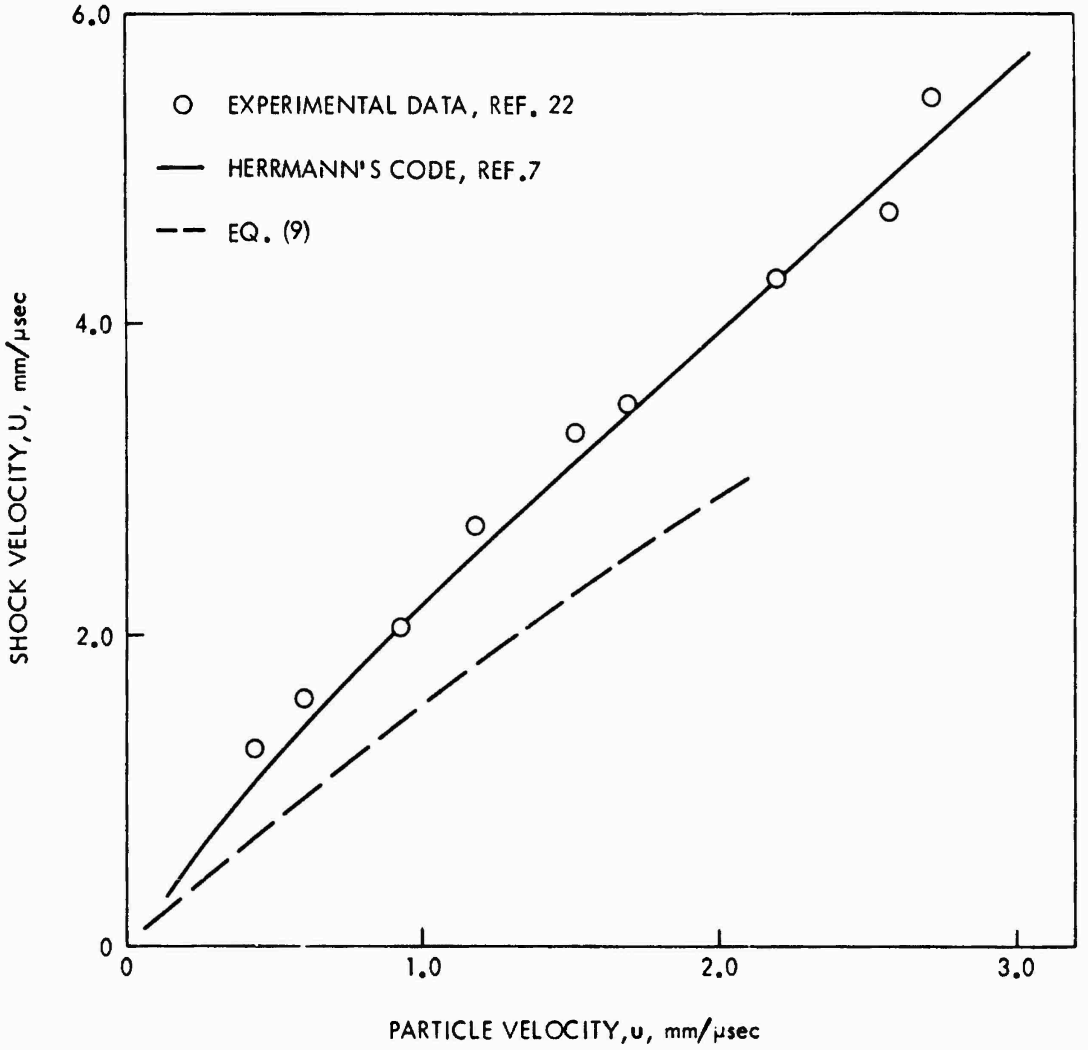

FIG. 11 COMPARISON OF EXPERIMENTAL AND COMPUTED HUGONIOTS FOR NB-40 AT 1.0 g/cc

what they call the "reflection technique" (i.e., impedance matching) is also plotted. They explain how the coincidence of the results of these two methods assures them that reaction has not affected their results. For tetryl, Figure 13, both computational models fit the experimental data very well. For PETN, Figure 14, our computations give values of U which are too small for given values of u, while the Russian computations follow their data. Again, we have not tried adjusting parameters to make the Herrmann model fit the data more closely. For AN, Figure 15, both computations give values of U which are too small.

The above comparisons are summarized in Table 5. The materials are listed in the left hand column of the table. The next column gives the density of the porous material used in the experimental work. The next three columns indicate (1) how our computations agree with the experimental data, (2) how the Russian calculations[10] compare with their own experimental data, and (3) how our computations compare with the Russian computations.

TABLE 5

COMPARISON OF COMPUTED AND EXPERIMENTAL RESULTS FOR SIX EXPLOSIVES

Material	Density g/cc	Our Calc. vs. Experimental Data	Russian Calc. vs. Experimental Data	Our Calc. vs. Russian Calc.
TNT	0.98	good	+	+
NB*	1.00	good	+	+
RDX*	1.00	good	good	good
tetryl*	0.86	good	good	good
PETN*	0.82	poor	good	poor
AN*	0.86	poor	poor	good

* Experimental work from Reference 10.

+ No results reported in Russian literature.

We conclude that our calculations fit the data at least as well as do the Russian calculations, which are much more involved. Hence, we see no need to use the more complicated computational method used by the Russians. For AN, the computations, in both cases, may be in error because of errors in the Hugoniot of the solid AN. This material changes phases under pressure so that the Hugoniot cannot be represented by a single linear relation between shock and particle velocities. Of course, the experimental data for AN, and for PETN, may also be in error even though the Russians tried to avoid letting reaction affect their results.

Up to this point in this report, we have used the Herrmann code to calculate the 0.98 g/cc Hugoniot for TNT only. Figures 16 and 17 give computed Hugoniots for TNT for densities from 1.0 to 1.60 g/cc.* In Appendix D we compare experimental results with the computed Hugoniot for TNT at 1.3 g/cc. Here we note that in Figure 16 the relation for 1.0 g/cc TNT is very nearly linear -- this is why equation (31) can be used. At greater initial densities (smaller values of α_o), the relations tend to become curved for small values of the particle velocity, that is, at low pressures. This is noticeable even for 1.60 g/cc TNT. Because we have not been able to compute the shock variables in the crushup regime, we cannot attach a great deal of importance to the curvature mentioned above. That is, if we had been able to compute the values of these variables in the crushup regime, the curvature may have been more or less than we show in Figures 16 and 17. Actually, our U,u curves resemble those published by Herrmann[7] in his Figure 2 which is for aluminum. In his calculations, he neglected the elastic response of the porous aluminum. For iron, the curves become more complex, see Figure 6 in Reference (7). In that work, Herrmann tried to account for the elastic response of the distended iron, and the crushup process. Hence, we should expect to obtain curves that are more complicated than those shown in our Figure 16 when we are able to account for the entire compaction process.

CONCLUSIONS AND FUTURE WORK

Our results show that Hugoniots for porous TNT can be calculated to a good degree of accuracy by using the mathematical model described by Herrmann[7]. Most of our work was with TNT at 0.98 g/cc; a small amount with TNT at 1.3 g/cc. Furthermore, we reproduce experimental Hugoniots given in the Russian literature[10,22] for NB, RDX, and tetryl to a good degree of accuracy. For PETN and for AN, our computations agree less well with the Russian data[10,22]. This failure may be due to inaccuracies in the Russian Hugoniot data on the low density forms of each material, or on the values of the parameters which the Russians use to describe the Hugoniots of the solids or a combination of these. The Russians themselves do not obtain close agreement between calculated and experimental Hugoniots for AN. This material is hygroscopic which makes it difficult to keep pure in experimental work. Also, it undergoes phase changes under pressure. For these reasons, the Hugoniots of porous AN may be difficult to model. In the case of PETN, a fairly sensitive explosive, reaction may have caused errors in the Russian experiments, especially with the porous forms of the explosive. These errors may exist in spite of the precautions employed by the Russians (see the previous section of this report).

*Tables A2 and A3 in Appendix A give values of some of the flow variables as functions of the specific volume, v, for TNT at densities ranging from 1.0 g/cc to 1.614 g/cc.

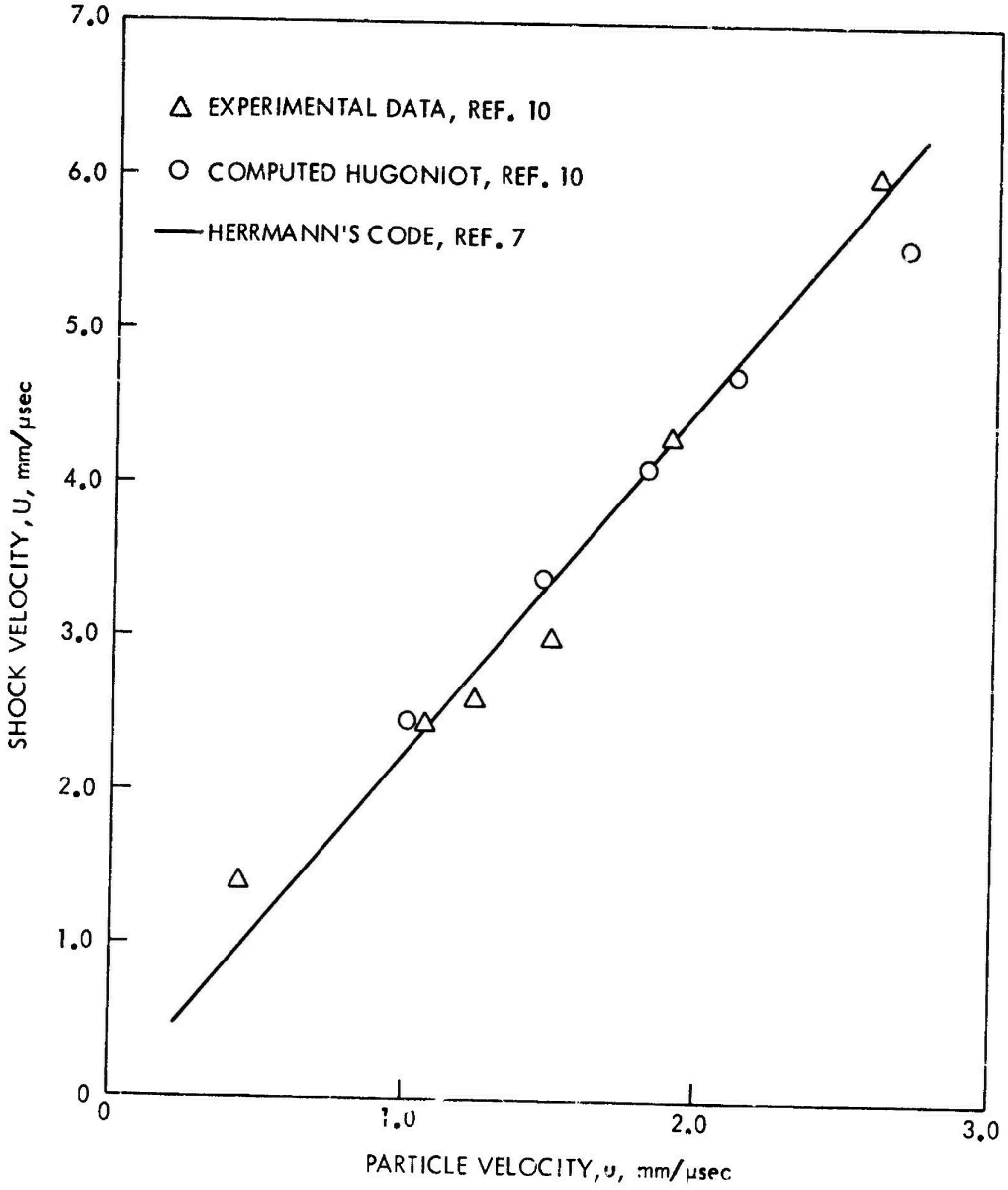

FIG. 12 COMPARISON OF EXPERIMENTAL AND COMPUTED HUGONICTS FOR RDX AT 1.0 g/cc

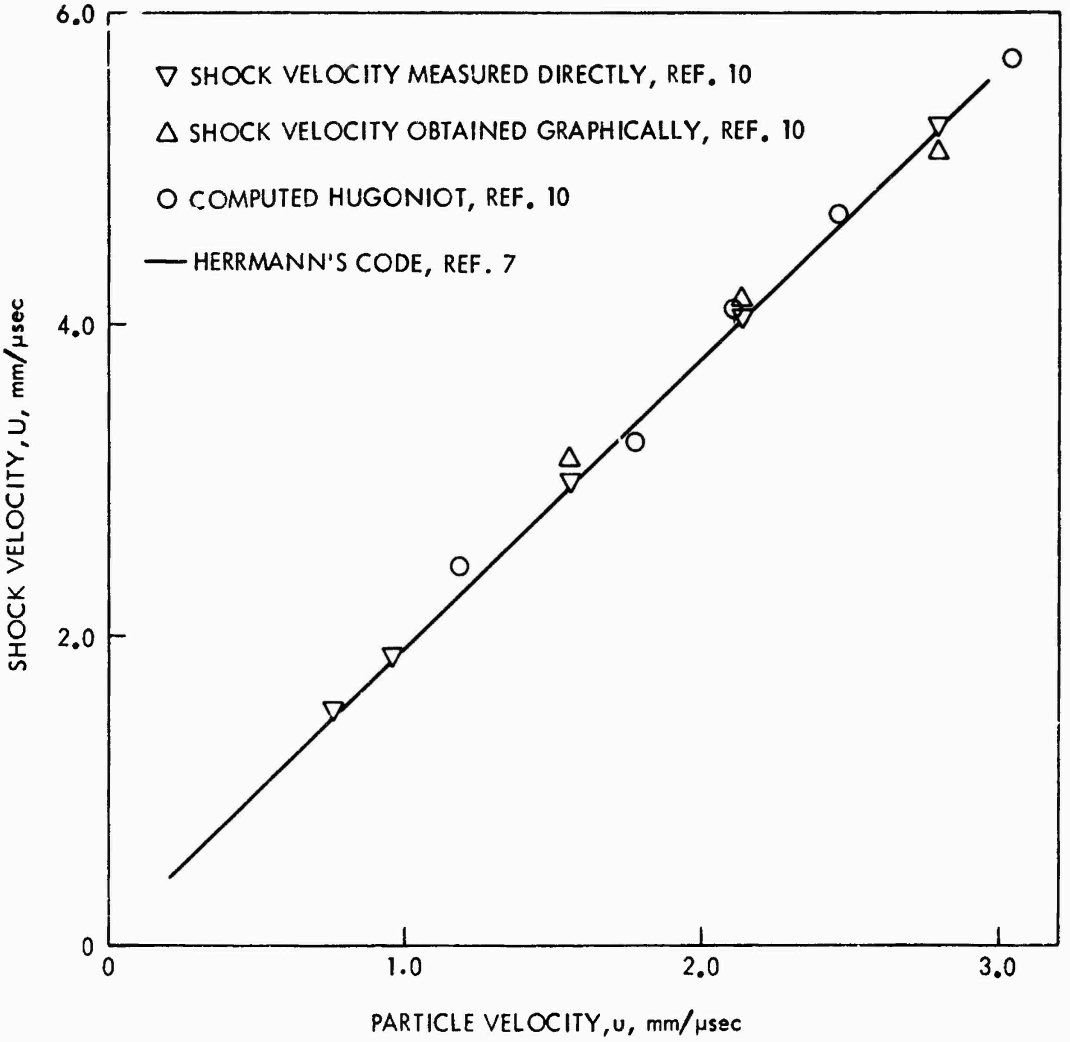

FIG. 13 COMPARISON OF EXPERIMENTAL AND COMPUTED HUGONIOTS FOR TETRYL AT 0.86 g/cc

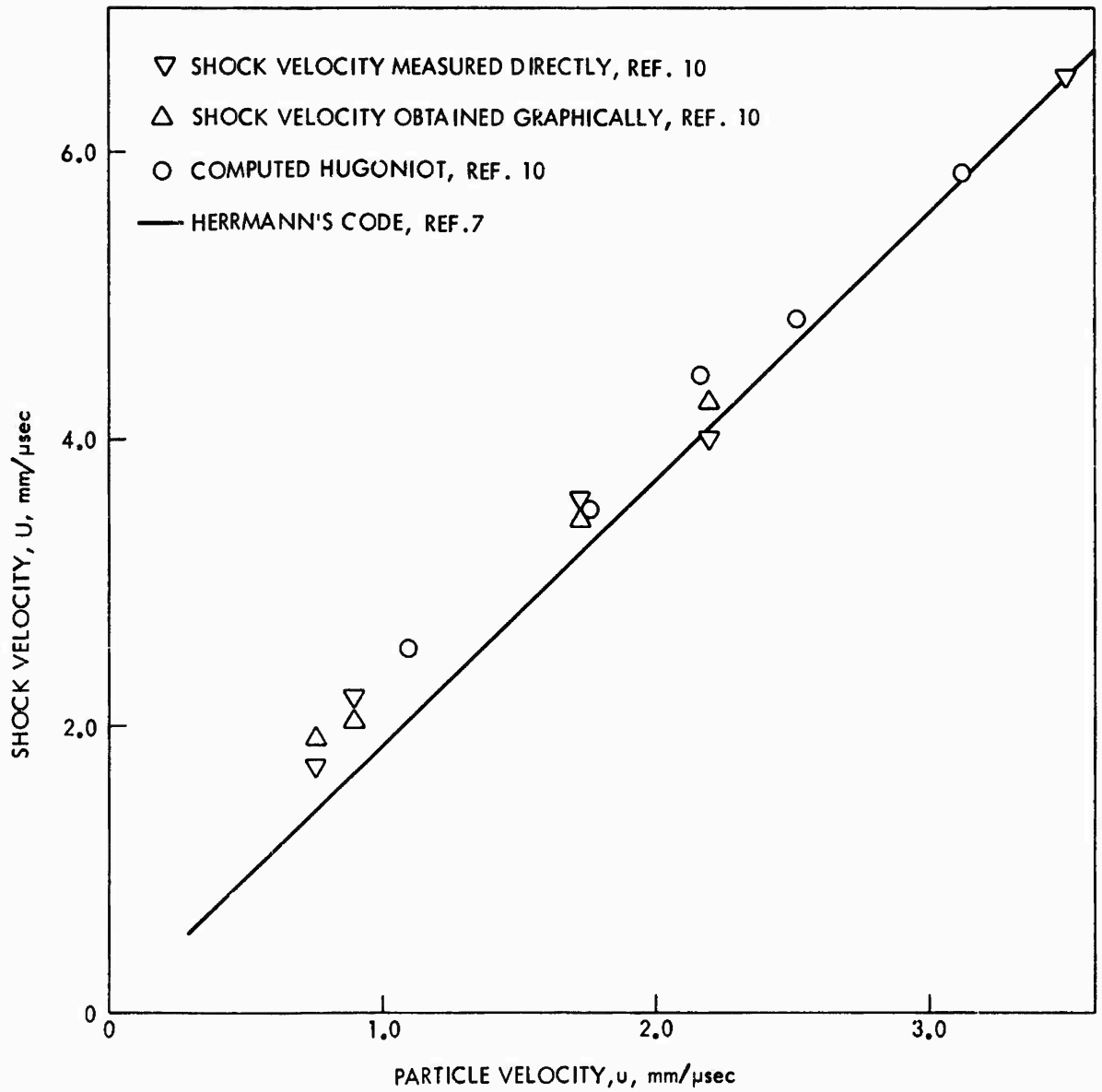

FIG. 14 COMPARISON OF EXPERIMENTAL AND COMPUTED HUGONIOTS FOR PETN AT 0.82 g/cc

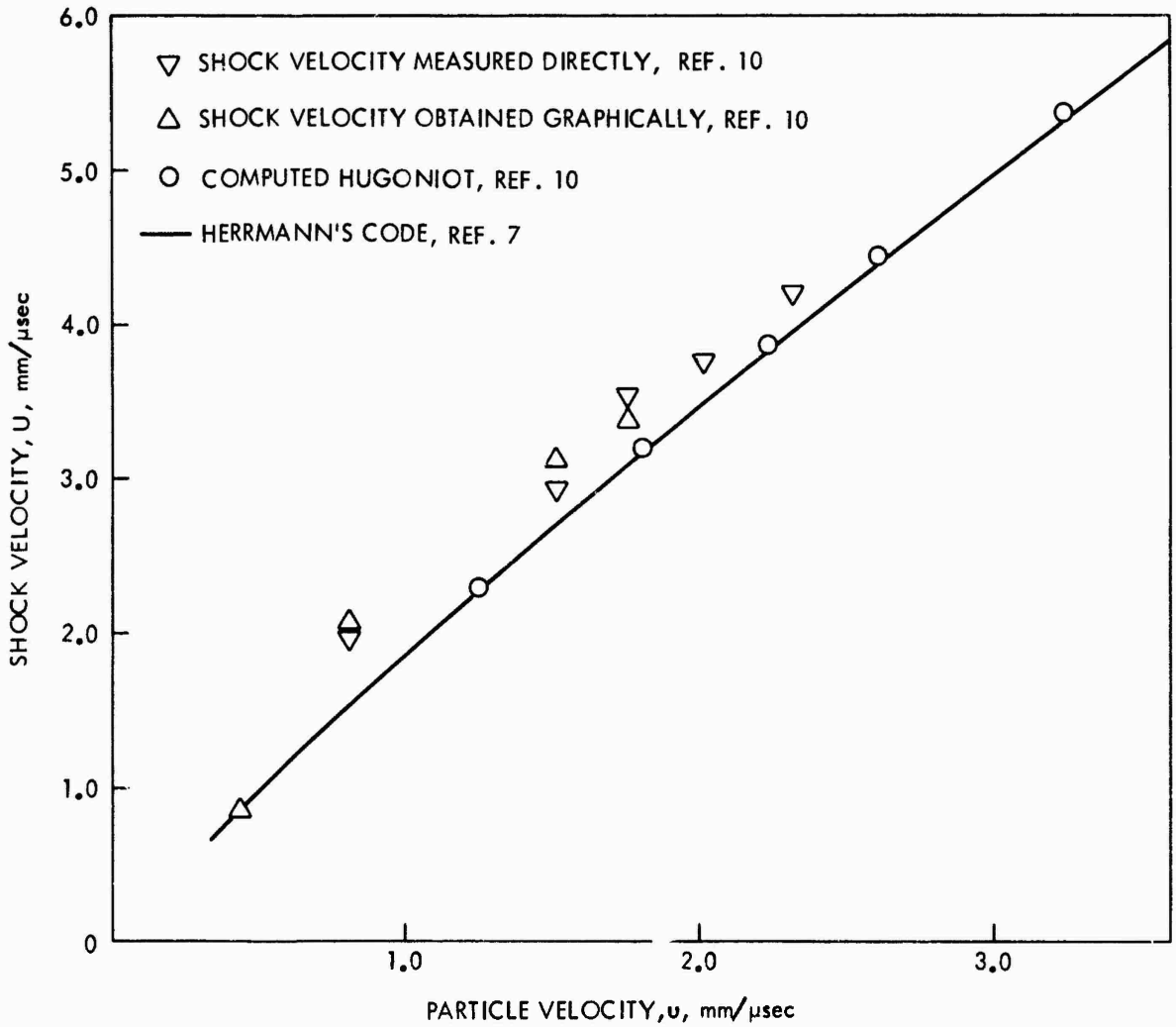

FIG. 15 COMPARISON OF EXPERIMENTAL AND COMPUTED HUGONIOTS FOR AN AT 0.86 g/cc

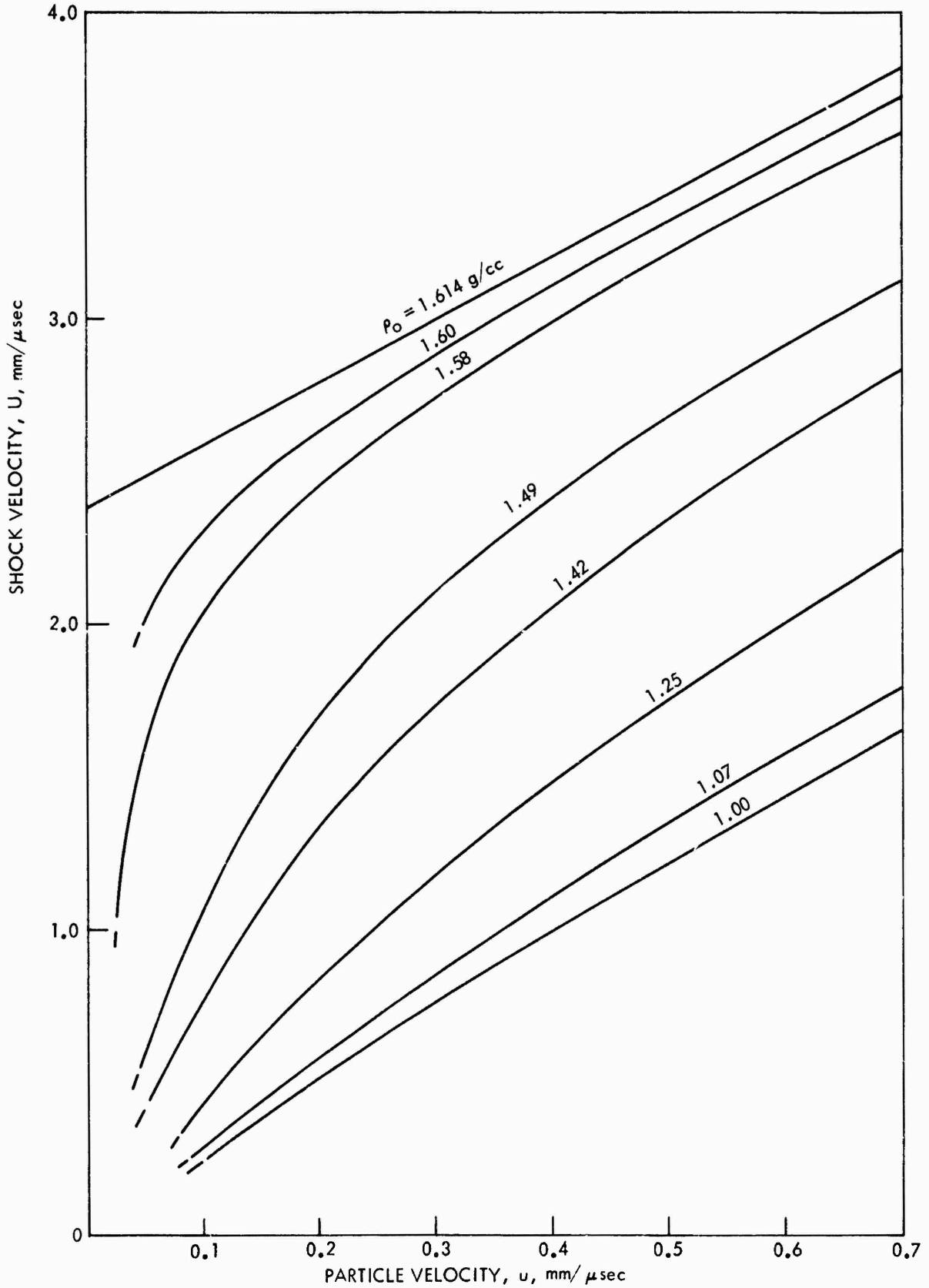

FIG. 16 SHOCK VELOCITY,U, VS PARTICLE VELOCITY,u, FOR TNT AT DIFFERENT DENSITIES

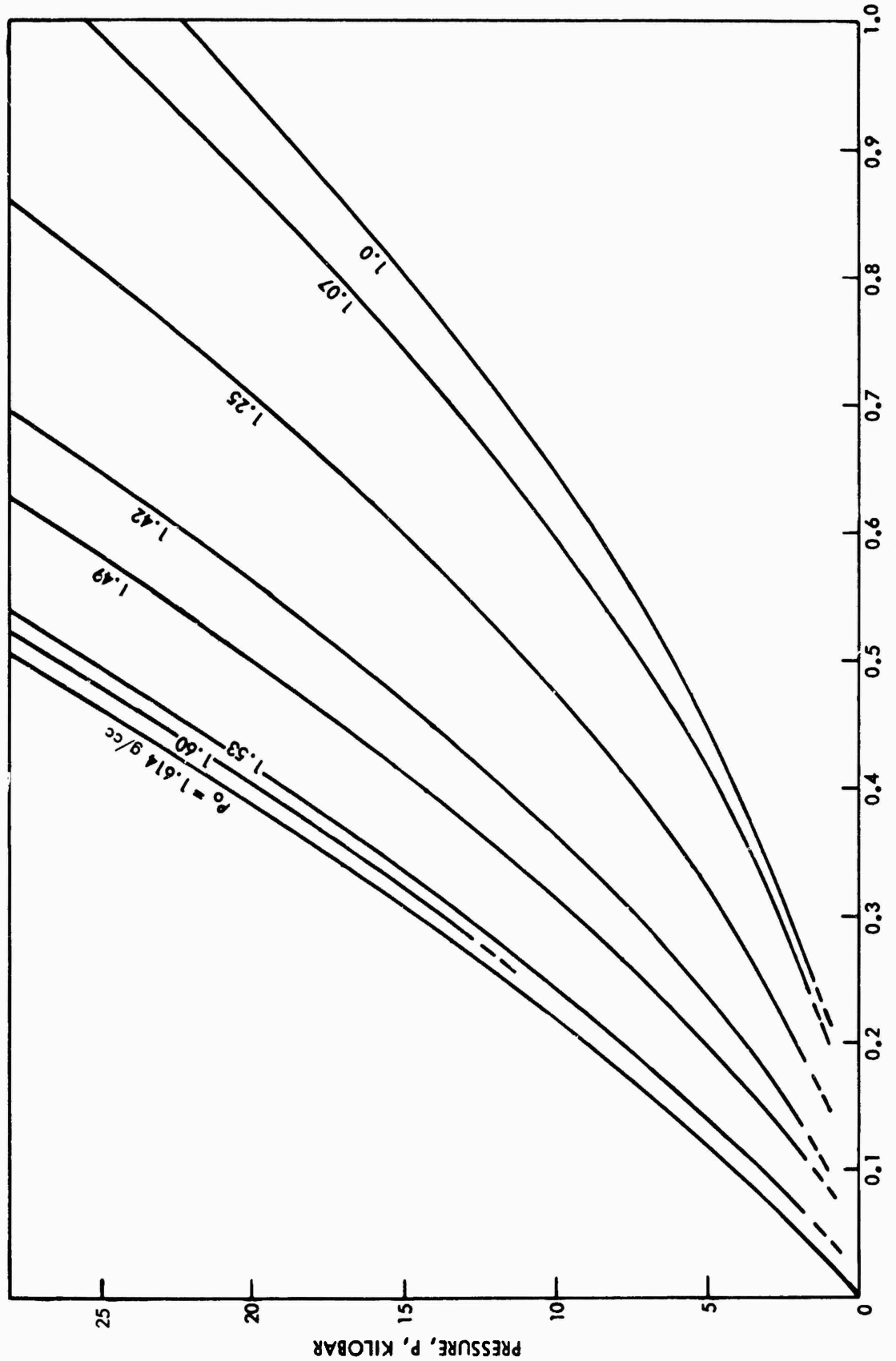

FIG. 17 PRESSURE VS PARTICLE VELOCITY FOR TNT AT DIFFERENT DENSITIES

The successes which we have reported above lead us to conclude that the mathematical model which we are using is adequate for predicting good approximations for the Hugoniots of porous explosives. It would be most surprising if the outcome had been negative. The model, and variations of the model, have been used successfully for years to describe the compaction of porous, unreacting solids by shock waves. The difficulty in working with explosives is, of course, their tendency to react when shocked. This challenges the experimentalist when he tries to acquire Hugoniot data for explosives in either their solid or porous form.

Otherwise, the degree of success in computing the Hugoniot for a porous explosive depends on the same factors as for an inert material. For example, if the explosive undergoes a phase change under pressure (hydrostatic or by shock), the model cannot be applied in the form now available to us. For example, the low melting point of TNT caused some ambiguity in the present study. If the solid material does not undergo a phase change under pressure (and the measurements are made before reaction can proceed to any significant degree in the experiment) the relation between the shock and particle velocities is apt to be linear as required by the simplified computer code reported in Appendix A. Curvature in the U,u relation for the solid can be handled by using a power series which relates the pressure to the volumetric strain, $\eta = (v_o - v)/v_o$, see reference (7).

The Gruneisen parameter of the solid material must be known. Studies of the same material in both solid and porous forms gives, in principle, values of the Gruneisen parameter, Γ. Our TNT data are too imprecise and too restricted in range for us to get any improvement in the value of Γ for TNT. The Russians, using this method, have given values of Γ for some explosives to pressures as great as 200 kbar. This is an extraordinary feat experimentally in view of the rapidity of the onset of reaction in most of these materials at these higher pressures. The value of Γ_o can be inferred from:

$$\Gamma_o = \alpha c_o^2 / c_p$$

where α is the volumetric thermal expansion coefficient, c_o is the ambient sound speed and c_p is the specific heat at constant pressure. For many solid explosives, reliable values of these parameters do not exist. Hence, determinations of c_p, c_o, and α are necessary supplementary work for successful use of the Herrmann Code.

A big part of the problem in the study of shock compression of porous media is what takes place when low amplitude shocks propagate through the material. We have not been able to deal with this problem in our TNT work, partly because of the experimental limitation which prevents us from producing low pressure shocks accurately and reproducibly. The potential simultaneous melting of the TNT also contributes to the problem of interpreting and using the data. Application of the mathematical models to the compaction region must wait until data are available on the elastic behavior of the porous materials. (Some of the relevant data can be obtained from sonic experiments.) Another

important parameter is the pressure at which the voids are essentially completely closed. For TNT, this measurement may have been obscured, we believe, by melting occurring simultaneously with the completion of crushup. It is most unfortunate that we do not have the data necessary to apply the computer models to the crushup process in explosives because the crushup pressure may be about the same as the critical pressure of the explosive in the large scale gap test (LSGT) for the very porous charges. Hence, we cannot convert our values of P_g (the pressure in the PMMA attenuator) to values of P_i, the critical pressure in the porous explosive because we could not obtain a reliable non-reactive explosive Hugoniot in this low pressure region.

No future work on the non-reacted Hugoniot of porous explosives is planned for two reasons. The first reason is that we have established the applicability of Herrmann's code to within the precision of our own (and the Russian) measurements in the pressure region of 10 - 55 kbar in this work and 10 - 100 kbar in the Russian work. The second reason is that the present experimental procedures are inadequate for studying the crushup region, i.e., the region below 10 kbar. The Russian researchers may also have problems in this region because they do not publish any data below 10 kbar.

Future work will involve the determination of non-reactive Hugoniots of voidless or near voidless high explosives for which no such data are now available. The explosives which will be studied should satisfy one or more of the following conditions.

1) The explosive dead-presses. That is, it will not propagate a detonation in the present experimental configuration.

2) A value for Γ_o (or the function $\Gamma(v)$) is available or can be determined for the explosive.

3) The explosive is used in the physical modeling of existing explosive mixtures or propellants.

SUMMARY

A theory of the response of porous materials to shock[5,6,7] which was found to apply to non-reactive materials, has been extended to a potentially reactive material, porous TNT. A computer code developed by Herrmann[7] and based on this theory used to calculate Hugoniots for unreacted TNT for the range of densities from 1.60 to 0.98 g/cc. The calculations were confirmed by obtaining an experimental Hugoniot for porous TNT at a density of 0.98 g/cc. The calculated and experimental Hugoniots agree to within 2 kbar over the range 0.35-1.72 mm/μsec and 3.6-55.0 kbar.

Thus, it appears that Hugoniots for unreacted, porous explosives can be obtained using a computational method (provided that a good Hugoniot is available for the near voidless unreacted explosive) with a high degree of confidence. This method results in a saving of time and money compared to the use of experimental method to obtain these Hugoniots.

REFERENCES

1. S. J. Jacobs, ARS Journal, 30 (2), 151 (1960)

2. Explosives Hazard Clasification Procedures, NAVORDINST 8020.3, p. 9

3. J. O. Erkman, D. J. Edwards, A. R. Clairmont, Jr., and D. Price, "Calibration of the NOL Large Scale Gap Test; Hugoniot Data for Polymethyl Methacrylate", NOLTR 73-15, 4 April 1973

4. David J. Edwards, John O. Erkman, and Sigmund J. Jacobs, "The Electromagnetic Velocity Gage and Application to the Measurement of Particle Velocity in PMMA", NOLTR 70-79, 20 July 1970

5. R. R. Boade, J. App. Phys., 39, 5693-5702 (1968)

6. R. Hofmann, D. J. Andrews, and D. E. Maxwell, J. App. Phys., 39, 4555-62 (1968)

7. W. Herrmann, J. App. Phys., 40, 2490-99 (1969)

8. L. B. Seely, J. H. Blackburn, B. O. Reese, and M. W. Evans, Comb. and Flame, 13, 375-91 (1969)

9. I. M. Voskoboinikov A. N. Afanasenkov, and V. M. Bogomolov, Comb., Expl. and Shock Waves, 3 (4), 359-64 (1967)

10. A. N. Dremin, K. K. Shvedov and O. S. Avdonin, Comb., Expl. and Shock Waves, 6 (4), 449-55 (1970)

11. L. V. Al'tschuler, K. K. Krupnikov, B. N. Ledenev, V. I. Zhuchikhin, and M. I. Brazhnik, Soviet Phys. JETP, 34 (4), 606-14 (1958)

12. Ya. B. Zel'dovich, Yu. P. Raizer, "Physics of Shock Waves and High Temperature Hydrodynamic Phenomena", Academic Press, New York 1966

13. I. V. Belinski and B. D. Khristoforov, "Dyna[illegible]mpressibility of Porous NaCl at Low Pressures", J. Appl. Mech and Tech. Phys., 11 (2), 318-323, March-April 1970

14. D. J. Edwards, to be published

15. A. Holt, A. Kusubov, M. Carroll, and B. Hord, "Stress-Wave Propagation in Distended Asbestos Phenolic", UCRL-51120, Lawrence Livermore Laboratory, 3 Sep 1971

16. R. Courant and K. O. Friedricks, "Supersonic Flow and Shock Waves", Interscience Pub., Inc., New York, 1948

17. K. W. Schuler and J. W. Nunziato, "The Dynamic Mechanical Behavior of Polymethyl Methacrylate", Sixth Inter. Congress of Rheology, Lyon, France, 1972 (preprints)

18. L. M. Barker and R. E. Hollenbach, J. App. Phys., 41 (10), 4208-26 (1970)

19. V. A. Vasil'ev, L. G. Bolkhovitinov, and B. D. Khrostoforov, Comb., Expl. and Shock Waves, 3 (4), 371 (1967)

20. A. N. Dremin, S. A. Koldunov, and K. K. Shvedov, Comb., Expl. and Shock Waves, 7 (1), 87-92 (1971)

21. N. L. Coleburn and T. P. Liddiard, Jr., "The Unreacted Hugoniot Equation of State of Several Explosives", Preprints, 4th Symp. on Detonation, 1965. (Also see J. Chem. Phys., 44, 1929 (1966))

22. V. A. Veretennikov, A. N. Dremin, and K. K. Shvedov, Comb., Expl. and Shock Waves, (4), 342-45 (1969)

23. V. M. Boyle, W. G. Smothers, and L. H. Ervin, "The Shock Hugoniot of Unreacted Explosives", 5th Symp. (Inter.) on Detonation, Pasadena, Ca., August 18-21, 1970

24. R. G. McQueen, S P. Marsh, J. W. Taylor, J. N. Fritz, and W. J. Carter, "The Equation of State of Solids from Shock Wave Studies", Chap. 6, High-Velocity Impact Phenomena, R. Kinslow, ed., Academic Press, New York, 1970

25. Engineering Design Handbook, Explosives Series, "Properties of Explosives of Military Interest". AMCP No. 706-177, January 1971.

APPENDIX A

COMPUTER CODE FOR CALCULATING HUGONIOTS FOR POROUS SOLIDS

The computer code given by Herrmann has the option for computing the pressure of a porous material in the crushup region. Actually, the major part of that code consists of the crushup option. All that is needed for the work which we have reported is a means of computing values from Equations 4 and 8 of the main text. A code for doing this is given in Table A1. It is written in CDC Fortran, and is designed to run from a teletype terminal using CDC "INTERCOM" System. Input to the code is accomplished by using an "INPUT" statement. The code asks for input data as shown on the first line in Table A2. These are values for c_o and S, see Equation 5, Γ_o, the initial porosity parameter, α_o, i.e., v_{of}/v_{os}, and finally v_{os}. In the code, these variables are named CO, S, GO, AO, and VS, respectively. The data are immediately printed out by the computer for checking by the operator. Three quantities are given on the next line in Table 2. The first is the value of VS, the specific volume of the solid. The second is that at which P_f goes to infinity, see equation 4 in the main text. The difference, VS - V2, is divided by 40 to give an increment in the specific volume for the following computation. This increment, V3, is used in a "DO" loop to increment the specific volume 20 times, or until PP, i.e., P_f, exceeds 0.1 megabar (for some runs, the test value was 0.175 megabars).

The tabular output of the code consists of:

V, the specific volume of the shocked material, i.e., v,

PH, the pressure in the solid at specific volume, i.e., P_s,

PP, the pressure in the porous material at specific volume v, i.e., P_f,

U8, the shock velocity, i.e., U,

U9, the particle velocity, i.e., u,

EI, the change in the internal energy due to the shock, given by $P_f(v_{of} - v) \times 1.195 \times 10^4$.

The change in internal energy (EI above) can be used to obtain a first approximation to the temperature jump across the shock by dividing by the specific heat. When a table is completed, the computer asks for a new set of data.

Units used in the code are cm/μsec for velocities (in contrast to the use of mm/μsec in the main text), cm^3/g for volume, megabars for pressure and cal/g for energy.

Table A3 gives the results of the code for TNT at densities of 1.07, 1.25, 1.42, 1.49, 1.58, 1.60, and 1.614 g/cc. The last density is that of TNT in what we regard in this report as the solid form. Consequently, the values of PH and PP (i.e., P_s and P_f) are identical for the same value of v. Part of the results given in Table A3 are displayed in Figures 16 and 17 in the main text.

Table A4 gives the results of the computations on which Figures 11 through 15 are based; the input data and its sources are given in Table 4 of the main text. An interesting feature of Table A4 is the results for RDX at 1.0 g/cc. The increment in the volume, Δv, turned out to be negative - the code extrapolates the solid Hugoniot into the tension region, hence the values of PH are negative. The values of PP (i.e., P_f) are positive, so that the v vs P_f curve has positive slope rather than negative slope. This behavior is inherent in the model and has been observed experimentally in some materials.

TABLE A1

COMPUTER CODE FOR CALCULATING HUGONIOTS FOR POROUS SOLIDS

```
100 PROGRAM HUG220 (INPUT,OUTPUT)
102 40 PRINT 600
104 PRINT 650
106C TYPICAL VALUES ARE 0.239, 2.05, 0.737, 1.614, 0.62
108 READ 660,C0,S,G0,A0,VS
110 PRINT 660, C0,S,G0,A0,VS
112 VF = A0 * VS
114 PRINT 600
116 F = 40.0
118 V2 = VS * A0 / (1.0 + 2.0 /G0)
120 V3 = (VS - V2) / F
122 V = VS
124 PRINT 500,VS,V2,V3
126 PRINT 600
128 PRINT 800
130 DO 30 I = 1,20
132 PH = C0 * C0 * (VS - V) / (VS - S * (VS - V))**2
134 PP = PH * (1.0 - G0 * (VS -V) * 0.5 / V)
136 PP = PP / (1.0 - 0.5 * G0 * (A0 * VS - V) / V)
138 U8 = VF * SQRT(PP / (VF - V))
140 U9 = SQRT (PP * (VF - V))
142 EI = 1.195E4 * U9**2
144 PRINT 700,V,PH,PP,U8,U9,EI
146 IF (PP .GE. 0.1) GO TO 40
148 V = V - V3
150 30 CONTINUE
152 500 FORMAT (3F10.4)
154 600 FORMAT (1H )
156 650 FORMAT(1H,*TYPE VALUES OF C0, S, G0, A0 AND VS, FORMAT F8.4*)
158 660 FORMAT (5F8.4)
160 700 FORMAT (3F10.4,2F10.3,F10.1)
162 800 FORMAT (5X,*V*,9X,*PH*,8X,*PP*,8X,*U8*,8X,*U9*,8X,*EI*)
164 END
```

TABLE A2

OUTPUT OF CODE LISTED IN TABLE A1
(TNT AT 1.0 G/CC, A0 = 1.614)

TYPE VALUES OF CO, S, GO, AO, AND VS
0.239 2.050 0.737 1.614 0.62
.2390 20500 .7370 1.6140 .6200
.6200 .2695 .0088

V	PH	PP	U8	U9	EI
.6200	0.0000	0.0000	0.000	0.000	0.0
.6112	.0014	.0018	.068	.026	8.4
.6025	.0029	.0038	.098	.039	18.3
.5937	.0047	.0062	.123	.050	30.0
.5849	.0067	.0088	.146	.061	43.9
.5762	.0089	.0119	.167	.071	60.3
.5674	.0114	.0154	.189	.082	79.7
.5587	.0143	.0194	.210	.093	102.6
.5499	.0177	.0241	.231	.104	129.9
.5411	.0214	.0295	.254	.117	162.2
.5324	.0258	.0359	.277	.130	200.8
.5236	.0309	.0433	.302	.144	246.9
.5148	.0367	.0521	.328	.159	302.3
.5061	.0436	.0625	.356	.176	369.1
.4973	.0516	.0748	.386	.194	450.1
.4885	.0611	.0897	.419	.214	549.0
.4798	.0724	.1077	.455	.237	670.5
.4710	.0860	.1297	.495	.262	821.1
.4623	.1024	.1569	.540	.291	1009.3
.4535	.1225	.1907	.591	.323	1247.0

TYPE VALUES OF CO, S, GO, AO, AND VS

TABLE A3

COMPUTED HUGONIOTS FOR TNT AT 7 DENSITIES

C0 = 0.239, S = 2.05, G0= 0.737, A0 = 1.5084, VS = 0.62
DENSITY = 1.07 G/CC

V	PH	PP	U8	U9	EI
.6200	0.0000	0.0000	0.000	0.000	0.0
.6108	.0015	.0018	.070	.024	7.0
.6016	.0031	.0039	.101	.036	15.4
.5924	.0050	.0062	.126	.046	25.4
.5832	.0071	.0089	.149	.056	37.5
.5740	.0095	.0120	.171	.066	51.9
.5648	.0123	.0156	.192	.076	69.1
.5556	.0155	.0198	.213	.087	89.7
.5464	.0191	.0246	.235	.098	114.4
.5372	.0233	.0303	.258	.110	144.1
.5280	.0283	.0369	.282	.123	179.8
.5188	.0340	.0448	.307	.137	223.0
.5095	.0407	.0541	.334	.152	275.4
.5003	.0487	.0653	.362	.169	339.4
.4911	.0581	.0788	.394	.187	417.9
.4819	.0695	.0951	.428	.208	515.0
.4727	.0831	.1151	.467	.231	636.0
.4635	.0998	.1398	.509	.257	788.3
.4543	.1204	.1709	.557	.287	981.9
.4451	.1461	.2102	.613	.321	1231.3

C0 = 0.239, S = 2.05, G0= 0.737, A0 = 1.2912, VS = 0.62
DENSITY = 1.25 G/CC

V	PH	PP	U8	U9	EI
.6200	0.0000	0.0000	0.000	0.000	0.0
.6099	.0016	.0018	.078	.019	4.1
.5998	.0035	.0039	.111	.028	9.3
.5897	.0056	.0063	.138	.036	15.9
.5796	.0080	.0091	.162	.045	24.0
.5694	.0108	.0123	.185	.053	34.0
.5593	.0141	.0161	.207	.062	46.4
.5492	.0179	.0205	.229	.072	61.7
.5391	.0224	.0258	.251	.082	80.5
.5290	.0277	.0320	.275	.093	103.7
.5189	.0339	.0393	.299	.105	132.4
.5088	.0413	.0482	.325	.119	168.0
.4987	.0503	.0589	.354	.133	212.5
.4886	.0611	.0720	.385	.150	268.4
.4784	.0743	.0881	.419	.168	339.0
.4683	.0907	.1081	.457	.190	429.2
.4582	.1111	.1334	.500	.214	545.7
.4481	.1371	.1657	.549	.242	698.0
.4380	.1705	.2078	.606	.274	900.2

TABLE A3 (CONTINUED)

C0 = 0.239, S = 2.05, G0= 0.737, A0 = 1.1366, VS = 0.62
DENSITY = 1.42 G/CC

V	PH	PP	U8	U9	EI
.6200	0.0000	0.0000	0.000	0.000	0.0
.6092	.0017	.0018	.097	.013	2.1
.5985	.0037	.0039	.135	.020	5.0
.5877	.0060	.0064	.164	.027	8.9
.5770	.0087	.0092	.189	.034	14.0
.5662	.0118	.0125	.212	.042	20.7
.5555	.0155	.0165	.234	.050	29.4
.5447	.0198	.0211	.256	.058	40.4
.5340	.0250	.0266	.278	.067	54.3
.5232	.0311	.0332	.302	.078	72.1
.5124	.0385	.0412	.326	.089	94.7
.5017	.0474	.0509	.353	.102	123.5
.4909	.0584	.0628	.382	.116	160.4
.4802	.0719	.0775	.414	.132	208.0
.4694	.0888	.0960	.450	.150	269.9
.4587	.1102	.1195	.491	.171	351.3
.4479	.1377	.1499	.538	.196	459.8
.4371	.1738	.1898	.594	.225	606.9

C0 = 0.239, S = 2.05, G0= 0.737, A0 = 1.0832, VS = 0.62
DENSITY = 1.49 G/CC

V	PH	PP	U8	U9	EI
.6200	0.0000	0.0000	0.000	0.000	0.0
.6090	.0018	.0018	.114	.011	1.4
.5980	.0038	.0039	.155	.017	3.4
.5871	.0062	.0064	.184	.023	6.4
.5761	.0089	.0092	.209	.030	10.6
.5651	.0122	.0126	.231	.037	16.1
.5541	.0160	.0166	.252	.044	23.3
.5431	.0205	.0213	.274	.052	32.7
.5322	.0259	.0269	.295	.061	44.9
.5212	.0324	.0337	.318	.071	60.6
.5102	.0402	.0419	.342	.082	80.8
.4992	.0497	.0519	.369	.095	106.9
.4883	.0615	.0642	.398	.109	140.7
.4773	.0761	.0796	.430	.124	184.9
.4663	.0944	.0990	.466	.143	243.0
.4553	.1180	.1239	.508	.164	320.3
.4443	.1486	.1564	.557	.189	424.7
.4334	.1892	.1996	.615	.218	568.2

TABLE A3 (CONTINUED)

C0 = 0.239, S = 2.05, G0= 0.737, A0 = 1.0215, VS = 0.62
DENSITY = 1.58 G/CC

V	PH	PP	U8	U9	EI
.6200	0.0000	0.0000	0.000	0.000	0.0
.6088	.0018	.0018	.172	.007	.5
.5975	.0039	.0039	.210	.012	1.7
.5863	.0063	.0064	.234	.017	3.6
.5751	.0092	.0093	.253	.023	6.5
.5638	.0126	.0127	.271	.030	10.6
.5526	.0166	.0167	.288	.037	16.2
.5413	.0213	.0216	.307	.045	23.7
.5301	.0270	.0273	.326	.053	33.7
.5189	.0339	.0343	.347	.063	46.9
.5076	.0423	.0427	.369	.073	64.2
.4964	.0525	.0531	.394	.085	86.9
.4852	.0652	.0660	.423	.099	116.8
.4739	.0812	.0822	.455	.114	156.5
.4627	.1015	.1028	.491	.132	209.6
.4515	.1278	.1294	.534	.153	281.3
.4402	.1624	.1646	.585	.178	379.8
.4290	.2092	.2121	.645	.208	517.8

C0 = 0.239, S = 2.05, G0= 0.737, A0 = 1.0088, VS = 0.62
DENSITY = 1.60 G/CC

V	PH	PP	U8	U9	EI
.6200	0.0000	0.0000	0.000	0.000	0.0
.6087	.0018	.0018	.206	.006	.4
.5974	.0039	.0039	.234	.010	1.3
.5861	.0064	.0064	.252	.016	3.0
.5748	.0093	.0093	.268	.022	5.6
.5636	.0127	.0127	.284	.028	9.4
.5523	.0167	.0168	.299	.035	14.7
.5410	.0215	.0216	.316	.043	21.8
.5297	.0273	.0274	.335	.051	31.4
.5184	.0342	.0344	.354	.061	44.0
.5071	.0427	.0429	.377	.071	60.7
.4958	.0531	.0534	.401	.083	82.7
.4845	.0661	.0664	.429	.097	111.8
.4732	.0823	.0827	.461	.112	150.5
.4619	.1030	.1036	.498	.130	202.4
.4507	.1299	.1306	.541	.151	272.8
.4394	.1655	.1664	.591	.176	370.0
.4281	.2136	.2148	.652	.206	506.6

TABLE A3 (CONTINUED)

C0 = 0.239, S = 2.05, G0= 0.737, A0 = 1.0000, VS = 0.62
DENSITY = 1.614 G/CC

V	PH	PP	U8	U9	EI
.6200	0.0000	0.0000	0.000	0.000	0.0
.6087	.0018	.0018	.248	.005	.2
.5973	.0039	.0039	.258	.009	1.1
.5860	.0064	.0064	.269	.015	2.6
.5747	.0093	.0093	.281	.021	5.0
.5634	.0127	.0127	.294	.027	8.6
.5520	.0168	.0168	.308	.034	13.6
.5407	.0216	.0216	.324	.041	20.5
.5294	.0274	.0274	.341	.050	29.7
.5181	.0345	.0345	.361	.059	42.0
.5067	.0430	.0430	.382	.070	58.2
.4954	.0535	.0535	.406	.082	79.7
.4841	.0666	.0666	.434	.095	108.2
.4727	.0831	.0831	.466	.111	146.2
.4614	.1041	.1041	.502	.128	197.3
.4501	.1314	.1314	.545	.149	266.9
.4388	.1676	.1676	.596	.174	363.0
.4275	.2167	.2167	.658	.204	498.6

TABLE A4

COMPUTED HUGONIOTS FOR 5 EXPLOSIVES USING RUSSIAN DATA

EXPLOSIVE - NB AT 1.00 G/CC
C0 = 0.170, S = 1.85, G0 =1.50, A0 = 1.63, VS = 0.6135

V	PH	PP	U8	U9	EI
.6135	0.0000	0.0000	0.000	0.000	0.0
.6043	.0008	.0015	.061	.024	6.9
.5950	.0016	.0032	.089	.036	15.4
.5858	.0025	.0052	.112	.046	25.8
.5765	.0036	.0076	.134	.057	38.6
.5673	.0048	.0105	.156	.067	54.4
.5580	.0061	.0140	.178	.079	74.0
.5488	.0077	.0182	.201	.091	98.4
.5395	.0094	.0235	.226	.104	129.1
.5303	.0114	.0299	.252	.119	168.0
.5210	.0137	.0381	.282	.135	218.1
.5118	.0162	.0486	.315	.154	283.5
.5025	.0192	.0623	.354	.176	370.5
.4933	.0227	.0808	.399	.202	489.4
.4841	.0267	.1066	.455	.235	657.2
.4748	.0315	.1442	.524	.275	905.0
.4656	.0370	.2029	.616	.329	1295.6

EXPLOSIVE - RDX AT 1.00 G/CC
C0 = 0.287, S = 1.61, G0 =2.60, A0 = 1.80, VS = 0.5556

V	PH	PP	U8	U9	EI
.5556	0.0000	0.0000	0.000	0.000	0.0
.5561	-.0001	.0034	.087	.039	18.0
.5566	-.0003	.0072	.127	.056	37.9
.5570	-.0004	.0113	.160	.071	60.1
.5575	-.0005	.0161	.191	.084	84.9
.5580	-.0006	.0214	.220	.097	113.0
.5585	-.0008	.0275	.250	.110	145.1
.5590	-.0009	.0345	.280	.123	181.9
.5595	-.0010	.0427	.311	.137	224.8
.5599	-.0011	.0524	.345	.152	275.4
.5604	-.0013	.0639	.381	.168	335.9
.5609	-.0014	.0781	.422	.185	409.8
.5614	-.0015	.0958	.467	.205	502.0
.5619	-.0016	.1185	.520	.228	620.4
.5624	-.0017	.1487	.583	.255	777.9
.5628	-.0019	.1911	.661	.289	998.3

TABLE A4 (CONTINUED)

EXPLOSIVE - TETRYL AT 0.86 G/CC
C0 = 0.217, S = 1.91, G0 =1.65, A0 = 2.012, VS = 0.5780

V	PH	PP	U8	U9	EI
.5780	0.0000	0.0000	0.000	0.000	0.0
.5754	.0004	.0024	.074	.037	16.6
.5728	.0008	.0051	.108	.055	35.6
.5702	.0012	.0081	.136	.069	57.4
.5675	.0016	.0116	.162	.083	82.4
.5649	.0020	.0156	.188	.097	111.4
.5623	.0025	.0202	.213	.110	145.2
.5597	.0029	.0257	.240	.124	185.0
.5571	.0034	.0321	.268	.139	232.2
.5545	.0039	.0398	.297	.156	289.0
.5519	.0044	.0491	.330	.173	358.3
.5492	.0049	.0606	.365	.193	444.2
.5466	.0055	.0751	.406	.215	553.0
.5440	.0061	.0939	.453	.241	694.6
.5414	.0067	.1192	.509	.272	885.5
.5388	.0073	.1549	.579	.311	1155.2
.5362	.0079	.2087	.671	.362	1563.0

EXPLOSIVE - PETN AT 0.82 G/CC
C0 = 0.242, S = 1.91, G0 =1.70, A0 = 2.159, VS = 0.5650

V	PH	PP	U8	U9	EI
.5650	0.0000	0.0000	0.000	0.000	0.0
.5648	.0000	.0030	.082	.044	23.1
.5645	.0001	.0062	.119	.064	48.8
.5643	.0001	.0099	.150	.081	77.6
.5641	.0002	.0141	.179	.096	110.1
.5639	.0002	.0188	.206	.111	147.0
.5636	.0003	.0241	.234	.126	189.2
.5634	.0003	.0303	.262	.141	238.0
.5632	.0003	.0376	.292	.157	295.0
.5630	.0004	.0462	.323	.174	362.4
.5627	.0004	.0565	.358	.193	443.5
.5625	.0005	.0691	.395	.213	542.6
.5623	.0005	.0848	.438	.236	666.7
.5621	.0006	.1051	.488	.263	826.4
.5618	.0006	.1322	.547	.295	1039.5
.5616	.0006	.1701	.620	.335	1338.0
.5614	.0007	.2270	.716	.387	1786.1

TABLE A4 (CONTINUED)

EXPLOSIVE - AN AT 0.86 G/CC
C0 = 0.220, S = 1.96, G0 =0.90, A0 = 2.012, VS = 0.5780

V	PH	PP	U8	U9	EI
.2200	1.9600	.9000	2.0120	.5780	
.5780	0.0000	0.0000	0.000	0.000	0.0
.5671	.0017	.0032	.085	.044	22.7
.5563	.0037	.0071	.126	.065	51.3
.5454	.0060	.0118	.161	.085	87.3
.5346	.0086	.0177	.195	.105	132.8
.5237	.0118	.0250	.230	.126	190.8
.5129	.0155	.0341	.266	.149	265.0
.5020	.0200	.0457	.306	.174	360.7
.4912	.0253	.0605	.349	.202	485.6
.4803	.0316	.0798	.398	.233	650.7
.4695	.0394	.1052	.453	.270	872.1
.4586	.0488	.1396	.518	.314	1175.0
.4477	.0605	.1871	.595	.366	1599.0

APPENDIX B

ESTIMATED ERRORS IN THE PRESSURE AND THE SPECIFIC VOLUME

As shown in the section on Impedance Matching, the pressure induced in the porous TNT is obtained graphically. Analysis of the error in such a process is difficult. A mathematical model would simplify the estimation of these errors. The impedance matching process can be described mathematically for the case in which the relief path in the P,u plane for the PMMA is a mirror image of the Hugoniot curve. Thus, to estimate errors we must ignore the viscoelastic effects on the unloading path for the PMMA. Because of the peculiar U,u relation for PMMA at pressures below about 20 kbar, the following analysis does not apply for low pressure work.

In the following, it is assumed that the relation between shock velocity, U and particle velocity, u, is linear, so that

$$U = c_o + Su, \tag{B1}$$

where velocities are in mm/μsec. This relation holds for pressures greater than 21.7 kbar in PMMA[3]. Note that when we have this pressure in the PMMA, we will have a considerably lower pressure in the approximately 1.0 g/cc TNT. Using the relation

$$P = 10\rho_o \, u \, U \tag{B2}$$

where ρ_o is the density (1.185 g/cc) of the unshocked PMMA, and P is the pressure in kbars, we have

$$P = 10 \, \rho_o \, u \, (c_o + S \, u) = A \, u + B \, u^2. \tag{B3}$$

The coefficients in equation B1 have the values 2.56 ± 0.01 mm/μsec and 1.595 ± 0.01 respectively[3], where the uncertainty is a standard deviation as given by a least squares fitting algorithm. Thus, the coefficients in equation B3, A and B, are 30.3 ± 0.1 and 18.9 ± 0.11 respectively.

The mirror image of the Hugoniot curve on the line $u = u_1$, see Figure 5 in the main text, is described by

$$P = A(2 \, u_1 - u) + B(2 \, u_1 - u)^2. \tag{B4}$$

The pressure corresponding to the particle velocity, u_1, is P_1. As shown in the section on Impedance Matching, we must locate the intersection of a curve described by Equation B4 with a line $u = u_e$, where u_e is the quantity measured by the EMV gage at the interface between the PMMA and the porous TNT. The pressure at the point where these curves cross is given by

$$P_e = A(2 \, u_1 - u_e) + B(2 \, u_1 - u_e)^2. \tag{B5}$$

The specific volume is given by

$$v_e = v_{of} - 10\, u_e^2/P_e \tag{B6}$$

where v_{of} is the initial volume of the porous material. We are concerned with the effect on the values of P_e and v_e of errors in the quantities A, B, u_1, u_e. We will assume that v_{of} is without error. Differentiating the above two equations gives

$$dP_e = dA(2u_1-u_e) + d\,B\,(2u_1-u_e)^2 + du_1(2A+4B(2u_1-u_e)) - du_e\,(A+2B(2u_1-u_e)), \tag{B7}$$

and

$$dv_e = 10u_e(u_e\, dP_e - 2P_e du_e)/P_e^2. \tag{B8}$$

Note that dP_e depends on four terms, each of which contains a differential of a variable or parameter which may be in error. As is conventional in error analysis, we replace the differentials by finite differences, and add the absolute values of the individual terms, giving,

$$\Delta P_e = |\Delta A(2u_1-u_e)| + |\Delta B(2u_1-u_e)^2| + |\Delta u_1(2A+4B(2u_1-u_e))| + |\Delta u_e(A+2B(2u_1-u_e))| \tag{B9}$$

and

$$\Delta v_e = 10u_e(|u_e\Delta P_e| + |2P_e\Delta u_e|)/P_e^2. \tag{B10}$$

Equations such as B8 and B9 usually overestimate the uncertainty in the error. Another way of combining the terms is to take the square root of the sum of the squares of the individual terms. In the following, such estimates will be indicated by placing a bar over the symbol representing the error, i.e., the estimated errors in P_e and v_e are $\overline{\Delta P_e}$ and $\overline{\Delta v_e}$ when this method is used.

In order to evaluate the errors as given by Equations (B9) and (B10) we need values of the estimated errors in A, B, u_1, and u_e. The estimated errors in A and B are given above--the values are from the computer code that was used to fit the linear expression, Equation B1, to the Hugoniot data of PMMA. The error in the particle velocity as measured by the EMV gage has been given before[3]. In that work, it was shown that the error in the particle velocity was made up of 7 components. The most important components were the error involved in reading the calibration marks on the oscilloscope record and in reading the oscilloscope trace itself. The total error was taken to be the sum of the absolute values of the seven terms. Using the nomenclature adopted above we are presenting Δu. The results are given in column 2 in Table B1. Note that there is some dependency of the error on the magnitude of the measured quantity. The variation is small, however. The reason for this is that the sensitivity of the oscilloscope is

TABLE B1

ESTIMATED ERRORS IN PARTICLE VELOCITY AS MEASURED WITH EMV GAGE

Particle Velocity, u mm/μsec	$\frac{\Delta u}{u} \times 100\%$	$\frac{\overline{\Delta u}}{u} \times 100\%$
0.1	6.2	3.1
1.0	5.7	3.0
2.0	5.6	3.0

changed so that approximately the same deflection is obtained for all velocities. In Reference 3 it was noted that the variation, such as it is, depends entirely on the 3 digit voltmeter which is used to calibrate the oscilloscope. The estimate of the error in the third column was obtained by taking the square root of the sum of the squares of the seven terms contributing to the error in the particle velocity. Again, using the nomenclature developed above, this quantity is identified as $\overline{\Delta u}$. The third column of Table B1 consists of values arrived at by this latter process. For these estimated errors, the variation with the magnitude of the particle velocity is negligible. Also, the estimated error is now considerably smaller, consistent with the expectation that some of the random errors should compensate for others. In the following we use ±3% as the error in the values of both u_1 and u_e and we proceed to evaluate Equations (B9) and (B10). This means we have changed Δu_1 and Δu_e in Equations (B9) and (B10) to $\overline{\Delta u_1}$ and $\overline{\Delta u_e}$.

We have chosen four pairs of values of u_1 and u_e from the raw data of Table 1 of the main text. These are listed in Table B2, along with the corresponding values of P_1 and P_e. Note that P_1 varies from 20.7 to 57.1 kbars, while P_e varies from 12.5 to 43.0 kbars, which covers the upper range of our data. The low pressure point, for which P_1 is 20.7 kbar, requires a small extrapolation of the linear U,u relation, Equation (B1); this introduces a negligibly small error in the value of P_1. The values, in kbars, of the individual terms of Equation (B9) are given in the columns headed E_1 through E_4. Note that both E_1 and E_2 are negligibly small. In the last column we show the square root of the sum of the squares of the 4 components of the errors, i.e., $\overline{\Delta P_e}$. These errors, which are in kbars, must be compared with the values of P_e which are given in column 5 of Table B2. We note that the magnitude of the error varies with the value of P_e. But the error on a percentage basis, see the last column of the table, does not vary significantly with the pressure. Apparently our error in the pressure in the test explosive is 12 to 13% over a range of pressure from 12.5 to 43.0 kbars in the low density TNT.

The error in the specific volume, v_e, of the shock compressed sample is computed from Equation (B10) in which ΔP_e and u_e are replaced respectively by $\overline{\Delta P_e}$ and $\overline{\Delta u_e}$. We have used the same pairs of values of

u_1 and u_e that we used for computing the error in the pressure, see Table B2. Equation (B6) is used to obtain the values of v_e, see the first column of Table B3. Values of P_e and $\overline{\Delta P_e}$ are from Table B2. In this case, the error has two components, labeled F_1 and F_2 in Table B3. The first component, that involving $\overline{\Delta P_e}$, dominates the second. Combining the errors by squaring, adding, and then taking the square root gives the expected error in volume, $\overline{\Delta v_e}$, see the next to last column in Table B3. In the last column, the errors are converted to percent relative errors. We have estimated errors ranging from about 7% to 13% in the data of Table 1, i.e., the raw data.

TABLE B2

ERROR IN THE PRESSURE, P_e

u_1	u_e	ρ_{of}	P_1	P_e	E_1	E_2	E_3	E_4	$\overline{\Delta P_e}$	% Error
mm/μsec		g/cc	kbar							
0.517	0.700	0.96	20.7	12.5	0.033	0.012	1.332	0.901	1.61	13.0
0.654	0.970	0.95	28.0	17.4	0.034	0.013	1.690	1.254	2.11	12.1
0.840	1.030	0.98	38.9	27.8	0.065	0.046	2.770	1.70	3.25	11.7
1.111	1.300	1.01	57.1	43.0	0.092	0.094	4.340	2.54	5.03	11.7

NOTE: By equation (B9), $\Delta P_e = \sum_{i=1}^{4} |E_i|$ which is not used here. The reported quantity is

$$\overline{\Delta P}_e = \sqrt{\sum_{i=1}^{4} E_i^2}$$

TABLE B3

ERROR IN THE SPECIFIC VOLUME

v_e	P_e	$\overline{\Delta P_e}$	F_1	F_2	$\overline{\Delta v_e}$	% Error
cc/g	kbar		cc/g			
0.650	12.5	1.61	0.050	-0.002	0.050	7.7
0.512	17.4	2.11	0.065	-0.002	0.065	12.8
0.639	27.8	3.25	0.045	-0.001	0.045	7.0
0.597	43.0	5.03	0.046	-0.001	0.046	7.7

NOTE:

By equation (B10)

$$\Delta v_e = |F_1| + |F_2|$$

By present treatment

$$\overline{\Delta v_e} = \sqrt{F_1^2 + F_2^2}$$

APPENDIX C

MELTING OF TNT UNDER SHOCK LOADING

Shock induced phase changes, such as melting, in materials are common. Boyle, Smothers, and Ervin[23] indicate that melting may occur in cast TNT, ρ_o = 1.62 g/cc, at around 32 kbar. In the section entitled "Comparison of Calculated and Experimental Hugoniot for Porous Explosives, Data from NOL and Other Sources", the possibility of melting of 0.98 g/cc TNT was raised as one explanation of the data points at P ~ 8.5 kbar, v = 0.795 cc/g, see Figure C1. In this appendix, this possibility will be discussed more fully.

If the TNT is melting at P ~ 8.5 kbar, v = 0.795 cc/g (or close to this point), the porous Hugoniot would have to be based on the parameters of liquid TNT. These are[23]

$$\rho_o = 1.472 \text{ g/cc} \qquad \text{(C1)}$$

$$U = 2.14 + 1.57\,u \quad , T = 81°C \qquad \text{(C2)}$$

where U and u are in mm/μsec. Γ_o is assumed to be the same as that for the solid, 0.737. The resulting Hugoniot is shown in Figure C1. As is evident from the figure, our data agrees with either Hugoniot equally well.

In shock loading studies, the usual procedures employed to detect a phase change are (1) determine if there is a break in the Hugoniot, and (2) determine if the initial wave splits into two waves. (An excellent discussion of shock induced phase changes is given by McQueen, Marsh, Taylor, Fritz, and Carter[24].) For 0.98 g/cc TNT, a break in the Hugoniot may exist at the above two mentioned data points. However, these data may also be due to crushup (or both). The temperature rise at these two data points can be calculated from the following equation

$$\Delta T = [1/2(P + P_o)(v_{of} - v) - H.F.]/c_v \qquad \text{(C3)}$$

where H.F. is the latent heat of fusion and is equal to 22.34 cal/g for TNT at 79°C[25], and c_v is the specific heat at constant volume and is equal to 0.29 cal/g/°C (see calculation of values of Γ_o in Ref. 21). ΔT for these two data points, using Equation (C3), are 60.9°C and 63.8°C. The initial temperature of the TNT was 25°C so that the final temperatures in the TNT were 85.9°C and 88.8°C. The melting point of TNT at ambient pressure is 81°C[25]. Thus, the melting of the TNT is a possibility if it is not strongly dependent on pressure.

In an effort to resolve this question, an attempt was made to detect multiple waves. Several experiments were performed with EMV gages located in the TNT at different distances from the PMMA/TNT interface. The length of the PMMA attenuator was 50.8 mm. The interface values of u_e and P_e were ~ 0.70 mm/μsec and ~ 12 kbar, respectively.

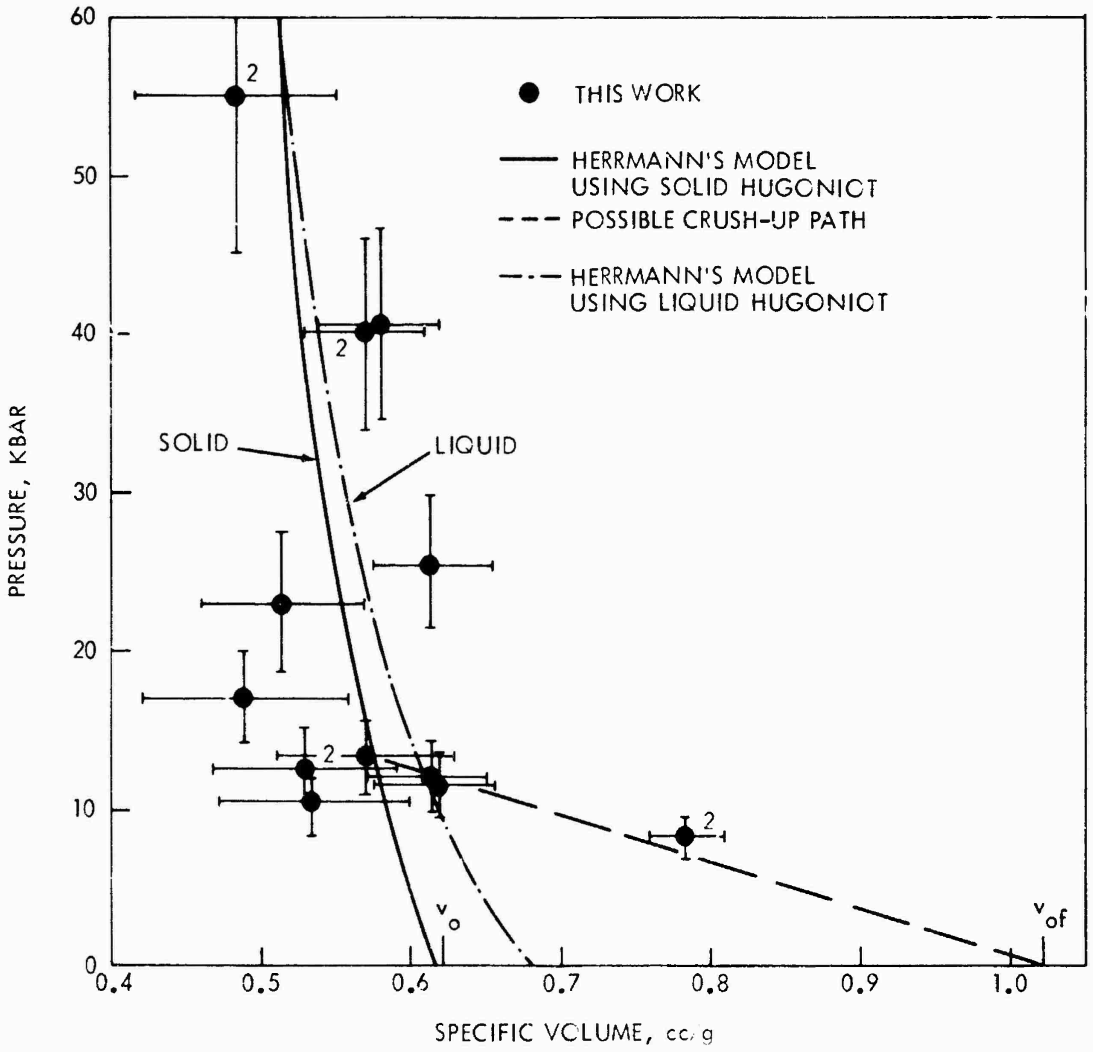

FIG. C1 P,v PLOT OF 0.98 g/cc TNT HUGONIOT

This is well above the values of the data which may indicate a phase change (i.e., at ~ 8.5 kbar) but below the Rayleigh line drawn through these data at ~ 8.5 kbar from v_{of}[24]. Thus, if a phase change is present in the vicinity of P ~ 8.5 kbar, u ~ 0.44 mm/μsec, and v = 0.795 cc/g, the wave should split for these initial interface values.

The u,t profiles generated by the EMV gage (with mica insulated leads) located in the TNT are shown in Figure C2. The number on each curve indicates the thickness in mm of the TNT between the PMMA/TNT interface and and the gage. One u,t profile from a gage located at 9 mm had a spurious electrical signal superimposed on it. This profile was smoothed by drawing a curve through the noise. This is the only profile which showed a hint of wave splitting. The other 9 mm profile (and an additional 9 mm profile not shown) have a faster risetime and reach a higher particle velocity than the interface (0 mm) result. These two facts indicate that buildup to detonation is occurring and eliminates any possibility of seeing wave splitting. Experiments at x > 9 mm also show buildup. Similar experiments were performed in 1.30 g/cc TNT but buildup to detonation was also present, see Appendix E. Because buildup to detonation occurs so rapidly in these experiments we have not been able to confirm or reject melting of the TNT at ~ 8.5 kbar.

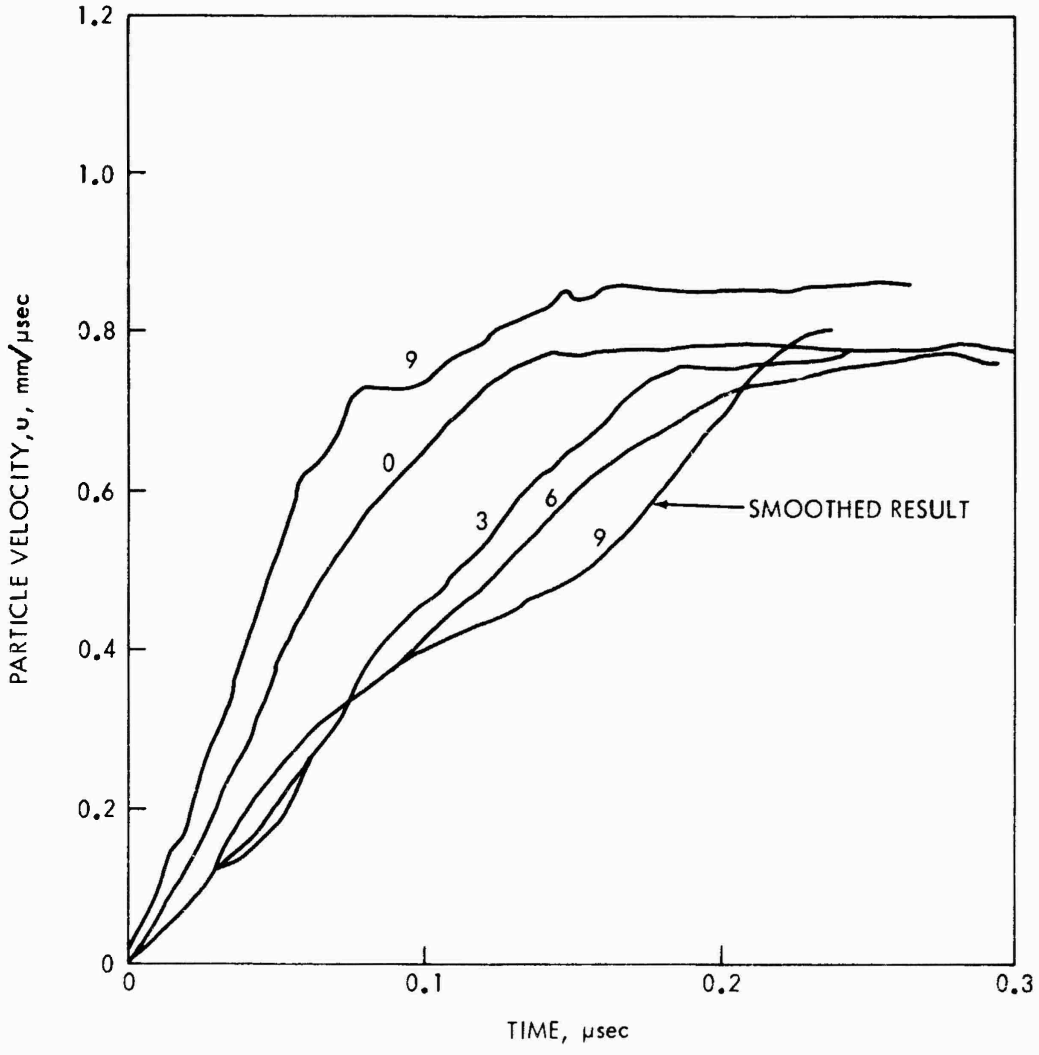

FIG. C2 u,t PROFILES AT VARIOUS LOCATIONS IN 0.98 g/cc TNT

APPENDIX D

SOME UNREACTED HUGONIOT DATA FOR TNT AT 1.30 G/CC

In the investigation of melting of TNT (see Appendix C), some experiments were performed in 1.30 g/cc TNT. These experiments had one EMV gage located at the PMMA/TNT interface and one EMV gage located in the TNT. The gages at the interface yielded unreacted Hugoniot data.

The u,t profiles obtained in 1.30 g/cc TNT showed an overshoot in u in the first 150 ns, see Figure D1. This overshoot was seen in PMMA[3] and is thought to be due to a piezoelectric effect. As was done in PMMA[3], the intercept particle velocity, u_e, was obtained by ignoring this overshoot and beginning the extrapolation at ~ 150 ns. The resulting u_e and P_e (obtained by impedance matching) are listed in Table D1 and plotted in Figure D2. Note that the scale of Figure D2 is ~ twice as large as earlier P,u plots. Because these data were close to the PMMA Hugoniot for forward facing shock (curve 1 of Figure 5), the correction due to viscoelasticity is small (~ 0.2 kbar) compared to the estimated error in pressure (2-3 kbar) and has been ignored. Also plotted in Figure D2 is the computed Hugoniot for 1.30 g/cc TNT obtained from Herrmann's model[7]. The agreement between the experimental data and the calculated Hugoniot is good.

TABLE D1

HUGONIOT DATA FOR 1.30 G/CC TNT

u_e mm/μsec	P_e kbar	U mm/μsec	v cc/g	Shot No.	u_1 mm/μsec	P_1 kbar	x mm
0.581	16.6	2.198	.566	344	.507	20.3	50.8
0.609	16.6	2.097	.546	343	.517	20.7	50.8
0.730	27.0	2.845	.571	342	.682	29.4	43.4

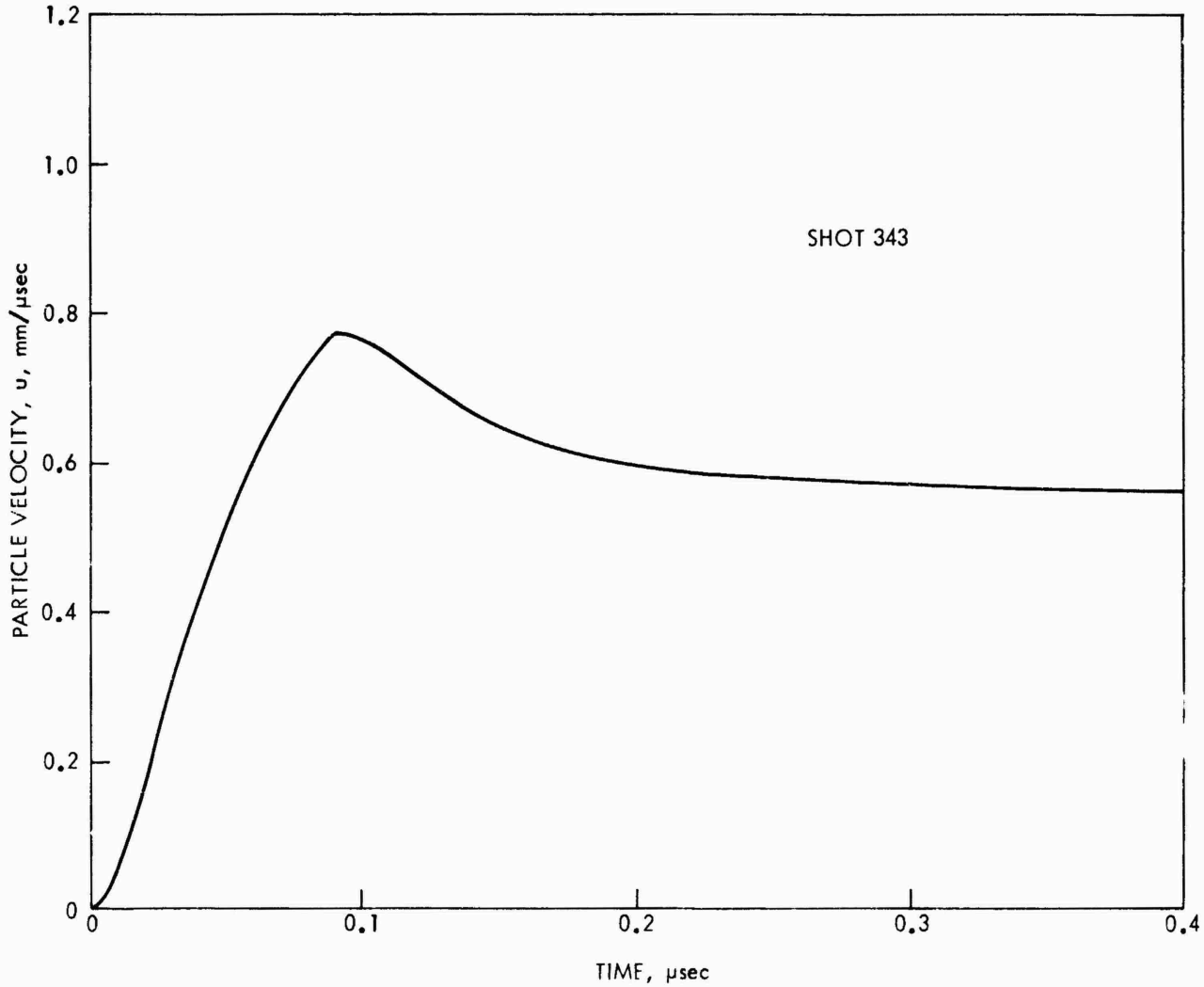

FIG. D1 u,t PROFILE AT INTERFACE OF PMMA/(1.3 g/cc) TNT

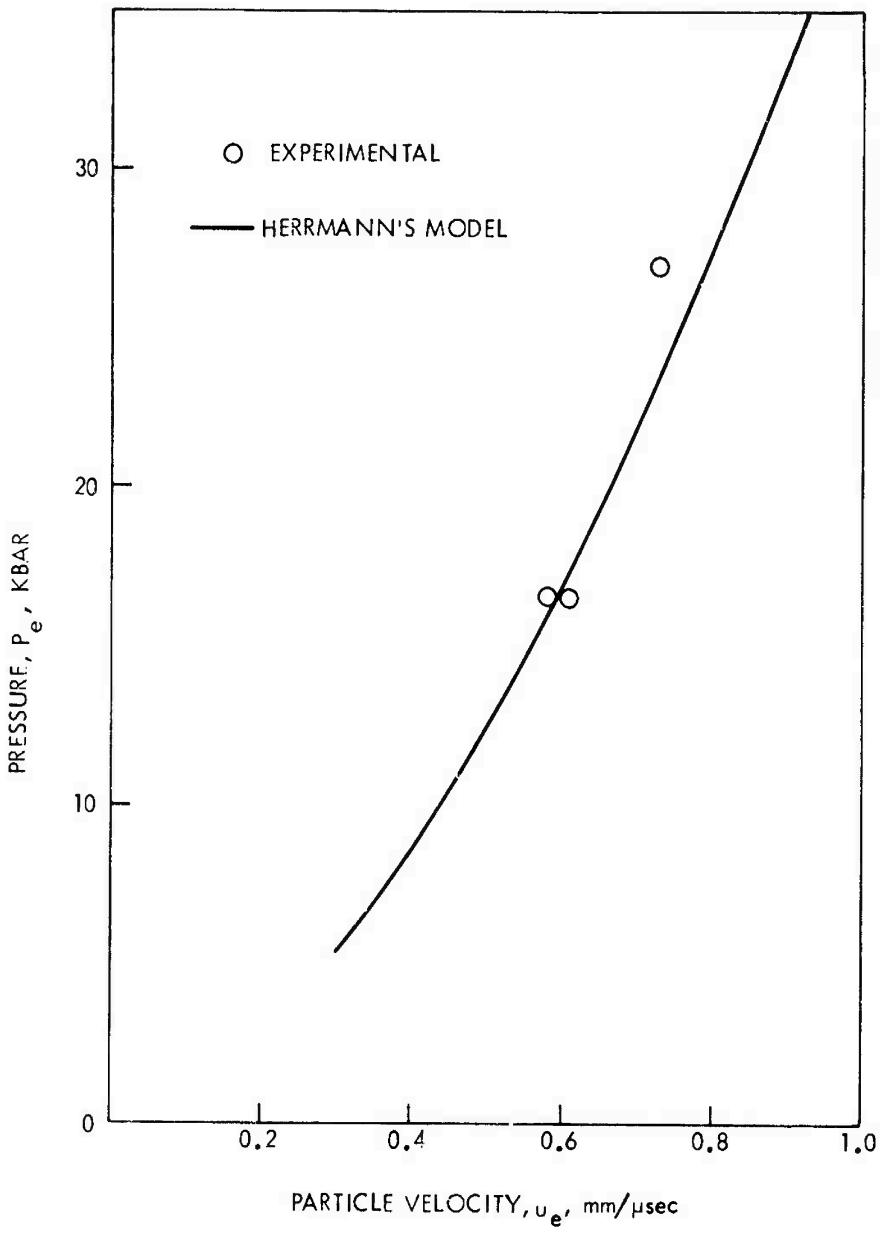

FIG. D2 P, u DATA FOR 1.30 g/cc TNT

APPENDIX E

BUILDUP OF PARTICLE VELOCITY IN LOW DENSITY TNT

When an explosive is subjected to a shock stimulus whose impulse is sufficiently large to cause eventual detonation but not great enough to cause immediate detonation, the particle velocity, shock velocity, and pressure will build up from their initial values to their steady state detonation values. The buildup of particle velocity in low density TNT as a function of ℓ, the distance from the inert/TNT interface to the gage, was obtained by using the experimental configuration shown in Figure 1 but with the EMV gages placed in the TNT at various locations. The buildup of particle velocity was investigated at two different initial pressures, P_e, in the TNT, ~ 40 kbar and ~ 12 kbar. The initial density was 0.98 g/cc ± 0.03 g/cc*. The quantity of interest is the initial value of the particle velocity, u_e. That is, the velocity at zero time of the gage record; this is not to be confused with u_{CJ} which occurs at some time $t > o$. This velocity is obtained by fitting the u,t result to a straight line by the method of least squares. The results are presented in Table E1. Some of the u,t curves obtained at various values of ℓ for the same initial pressure in the TNT, ~ 12 kbar, are plotted in Figure E1. Zero time on this figure is the zero time of the gage record. Note that as ℓ increases the peak of the particle velocity profile increases while the slope of the u,t curve after the peak, in most cases, becomes more negative. Reaction will cause this change in slope as will the gage leads being shorted out (see "Effects of Reaction on Gage Output"). The EMV gages used in the shots presented in Figure E1 did not have their leads encased in mica. Thus, the rapid falloff of the u,t curves is probably due to both effects.

Dremin, Koldunov, and Shvedov[20] have investigated the buildup of both particle velocity and shock velocity as a function of ℓ in 1.0 g/cc and 0.78 g/cc TNT and 0.82 g/cc tetryl using the EMV gage. At 1.0 g/cc Dremin investigated two different particle sizes of TNT, 0.1 mm and 0.37 - 1.0 mm. Since the large particle size used by Dremin is closer to the particle size of the TNT used here, only those data will be compared with ours. Instead of PMMA as the attenuator, Dremin used paraffin. The diameter of their charges was 60 mm while the diameter of the charges used in this study was 50.8 mm. The initial pressures in the Russian work were 8, 11.5, and 25 kbar. Dremin does not give any details on the type or density of high explosive booster he used. A different booster system will cause different buildup results. Results for the two higher pressures (open symbols) are compared with our results (solid symbols) in Figure E2. The Russian results were obtained from Figure 2 of Reference (20). At ~ 12 kbar, our results and Dremin's agree well. The buildup in particle velocity when P_e = 25 kbar obtained by Dremin appears to be more rapid than the buildup obtained in this study when

*Some data on the buildup of particle velocity in 1.30 g/cc TNT were also obtained. These data will be found at the end of Table E1.

P_e ~ 40 kbar. This may be due to the difference in charge diameter, particle size, and booster. The largest values of u_e obtained by Dremin is ~ 2.3 mm/μsec while the largest values observed here is ~ 2.2 mm/μsec. Again, this is probably due to the difference in charge diameter, particle size, and booster.

Dremin also obtained the relation between the shock velocity, U, and u_e in the partially reacting TNT at 1.0 g/cc. His result is

$$U = (0.30 + 1.85\ u_e)\ \text{mm/μsec.} \qquad \text{(E1)}$$

Equation (E1) is practically identical with our Equations (30) and (31) for non-reacting TNT at 0.98 g/cc.

TABLE E1

PARTICLE VELOCITY BUILDUP DATA FOR TNT

ℓ mm	u_e mm/μsec	ρ_o g/cc	Shot No.	Length of PMMA x, mm
		P_e ~ 40 kbar		
0.0	1.34	1.0	291	25.4
6.5	1.57	1.0	325A	25.4
25.0	2.10	1.0	321	25.4
50.0	2.19	1.0	322	25.4
50.0	2.18	1.0	323	25.4
77.0	----*	1.0	324	25.4
77.0	----*	1.0	329	25.4
		P_e ~ 12 kbar		
0.0	0.68	1.02	251	50.8
0.0	0.73	0.97	253	50.8
3.2	0.80	0.98	336	46.8
6.4	0.90	0.96	279	50.8
9.0	0.86	0.98	338m	50.8
9.0	0.80	0.98	339m	50.8
12.0	----**	0.98	338m	50.8
12.4	1.00	0.96	280	50.8
20.4	1.21	0.99	281B	50.8
20.4	1.27	0.96	285B	50.8
		P_e ~ 27 kbar		
0.0	.730	1.30	342	43.4
6.4	1.00	1.30	342	43.4
		P_e ~ 16.6 kbar		
0.0	.58	1.30	344	50.8
0.0	.61	1.30	343	50.8
6.4	~.67	1.30	344	50.8
12.4	~.80	1.30	343	50.8

* Noise on record.

** Risetime was same as total sweep of record.

m Mica covered gage leads.

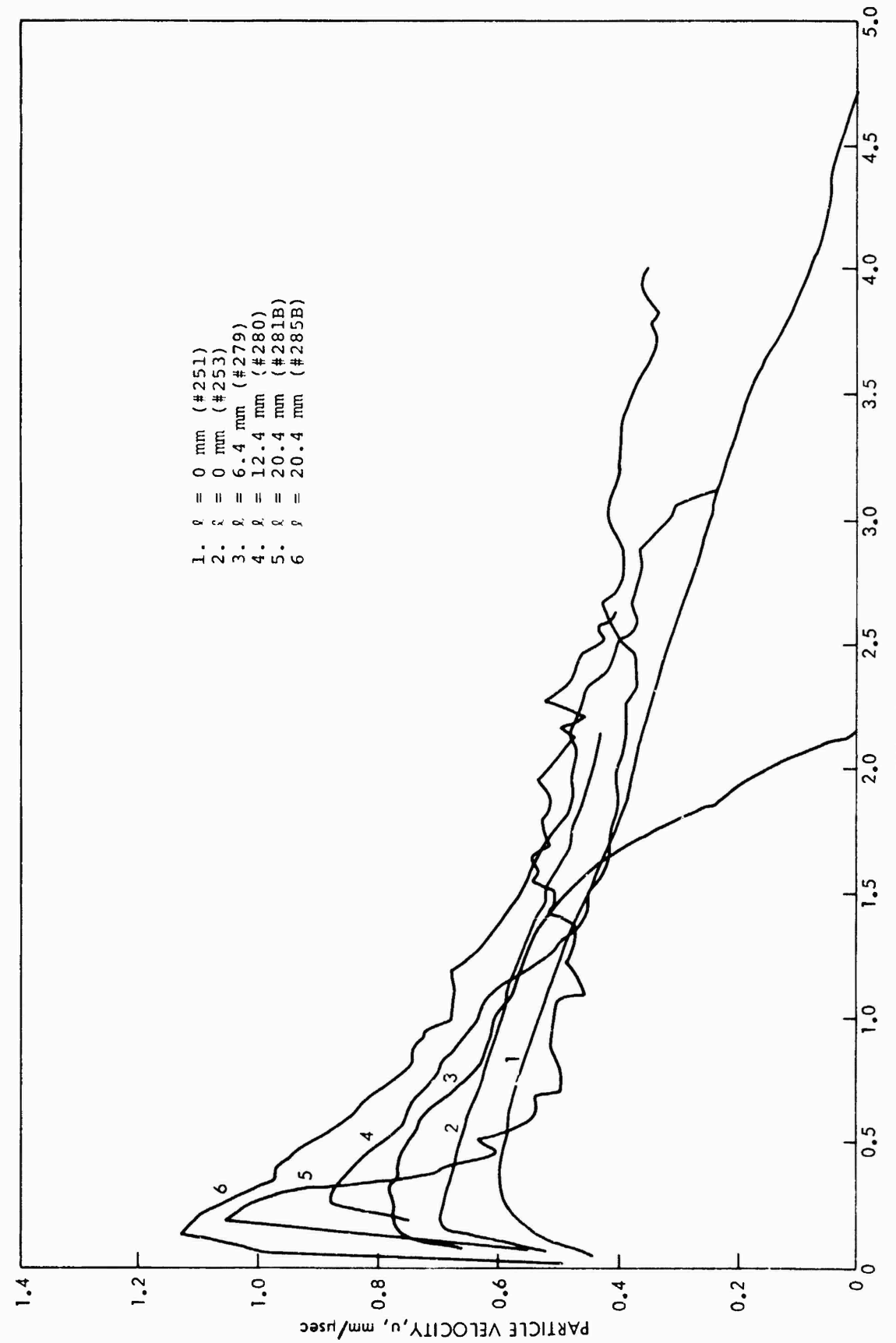

FIG. E1 COMPOSITE PLOT OF u,t CURVES (50.8 mm OF PMMA)

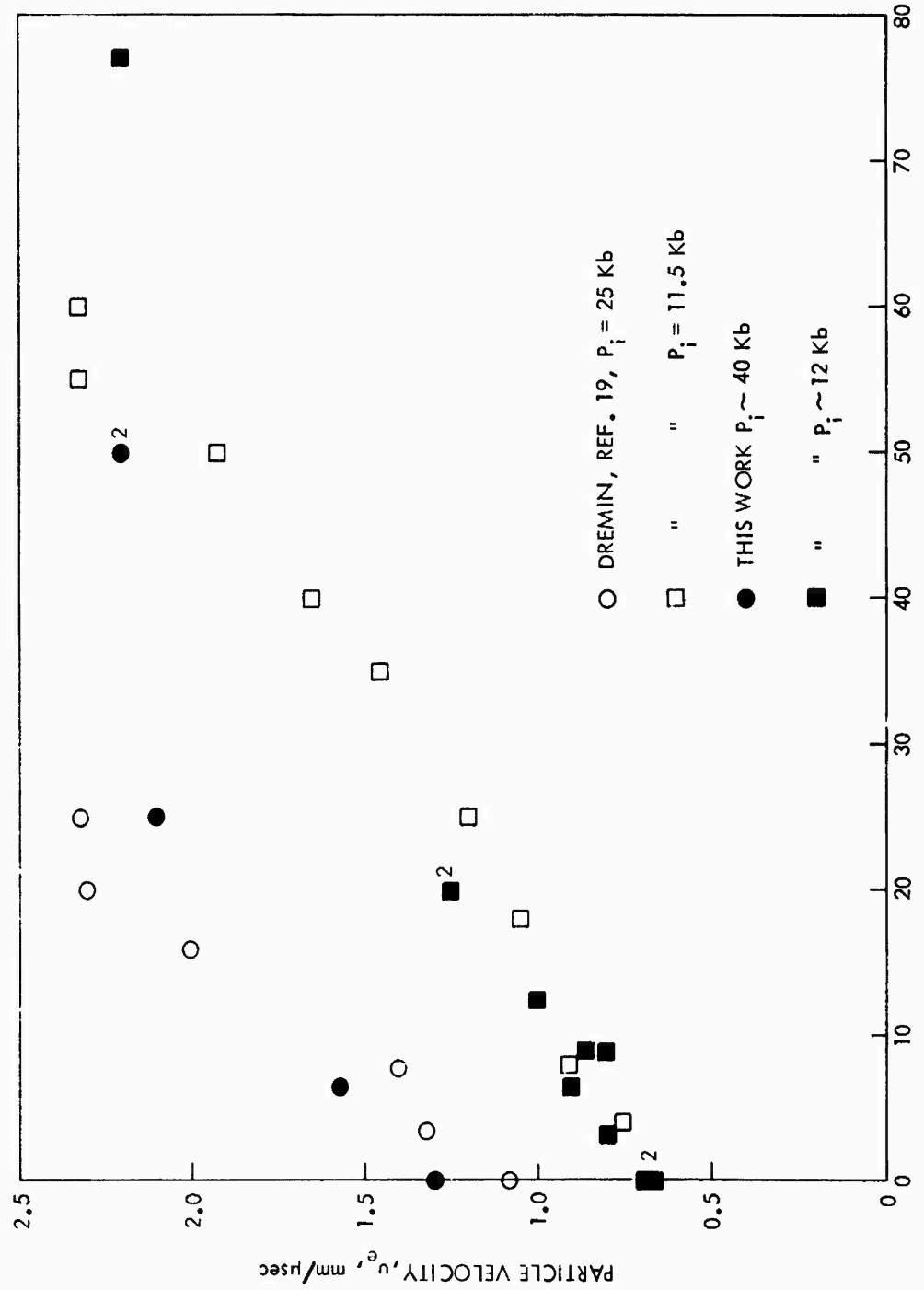

FIG. E2 COMPARISON OF BUILDUP DATA